[redacted]

A Reproduced Copy

OF

NASA MEMO 6-6-59A

Reproduced for NASA

by the

Scientific and Technical Information Facility

[redacted]

[redacted]

NASA MEMO 6-6-59A

6-22-59

NASA

MEMORANDUM

for

UNITED STATES AIR FORCE

STATIC STABILITY AND CONTROL CHARACTERISTICS OF A 0.5-SCALE MODEL OF THE HUGHES GAR-11 MISSILE AT MACH NUMBERS FROM 1.60 TO 2.30 (COORD. NO. AF-AM-162)

[redacted]

By Norman D. Wong and Rex R. Ellington

Ames Research Center
Moffett Field, Calif.

SERVICE REPORT

[redacted]

NATIONAL AERONAUTICS AND SPACE ADMINISTRATION

WASHINGTON

June 1959

16 pp

[redacted]

[redacted]

NATIONAL AERONAUTICS AND SPACE ADMINISTRATION

MEMORANDUM 6-6-59A

for

UNITED STATES AIR FORCE

STATIC STABILITY AND CONTROL CHARACTERISTICS OF A 0.5-SCALE MODEL OF THE HUGHES GAR-11 MISSILE AT MACH NUMBERS FROM 1.60 TO 2.30 (COORD. NO. AF-AM-162)*

By Norman D. Wong and Rex R. Ellington

ABSTRACT

Normal forces, axial forces, pitching moments, and rolling moments on the model and hinge moments on each of the four control surfaces were measured. Control surfaces were deflected from -35° to 15° in various combinations to produce pitching, yawing, and rolling moments on the model over a range of angles of attack from -5° to 25° at roll angles from -135° to 45°.

INDEX HEADINGS

Missiles, Specific Types	1.7.2.2
Stability, Longitudinal - Static	1.8.1.1.1
Control, Longitudinal	1.8.2.1
Control, Hinge Moments	1.8.2.5

*Title, Confidential

[redacted]

A-713

[redacted]

NATIONAL AERONAUTICS AND SPACE ADMINISTRATION

MEMORANDUM 6-6-59A

for

UNITED STATES AIR FORCE

STATIC STABILITY AND CONTROL CHARACTERISTICS OF A 0.5-SCALE MODEL OF THE HUGHES GAR-11 MISSILE AT MACH NUMBERS FROM 1.60 TO 2.30 (COORD. NO. AF-AM-162)*

By Norman D. Wong and Rex R. Ellington

SUMMARY

Normal forces, axial forces, pitching moments, and rolling moments on the model and hinge moments on each of the four control surfaces were measured. Control surfaces were deflected from -35° to 15° in various combinations to produce pitching, yawing, and rolling moments on the model over a range of angles of attack from -5° to 25° at roll angles from -135° to 45°.

INTRODUCTION

At the request of the Air Research and Development Command, United States Air Force, an investigation of the static stability and control characteristics of the 0.5-scale model of the Hughes GAR-11 missile was conducted in the three test sections of the Ames Unitary Plan wind tunnel. Six-component data, including hinge-moment measurements, were obtained. This report presents results obtained in the 9- by 7-foot test section at Mach numbers of 1.60, 2.00, and 2.30. Results obtained at Mach numbers from 0.8 to 1.4 and from 2.5 to 3.5 are reported in references 1 and 2. Various component configurations were investigated. In order to expedite the publication of the data, no analysis of the results is presented.

*Title, Confidential

[redacted]

[redacted]

COEFFICIENTS AND SYMBOLS

The system of axes and positive direction of forces, moments, and angles are presented in figure 1, which shows the coefficients referred to the balance axes. The moment center was located at model station 24.00. The coefficient C_A was adjusted for base force by an increment equal to the product of the base area (13.91 sq in.) times the difference between the measured base pressure and free-stream static pressure. In order to present the results in the same form as used for an earlier test of this missile (ref. 3), a reference body diameter of 3.20 inches and cross-sectional area of 8.04 square inches were used in the data reduction.

C_A axial-force coefficient, $\frac{\text{axial force minus base axial force}}{qS}$

C_{h_n} control surface hinge-moment coefficient, $\frac{\text{hinge moment}}{qSd}$

C_l rolling-moment coefficient, $\frac{\text{rolling moment}}{qSd}$

C_m pitching-moment coefficient, $\frac{\text{pitching moment}}{qSd}$

C_N normal-force coefficient, $\frac{\text{normal force}}{qS}$

C_n yawing-moment coefficient, $\frac{\text{yawing moment}}{qSd}$

C_Y side-force coefficient, $\frac{\text{side force}}{qS}$

d reference body diameter, 3.20 in.

M free-stream Mach number

q free-stream dynamic pressure

S reference body cross-sectional area, 8.04 sq in.

α angle of attack of balance axis, deg
(angle, in balance normal force or sting pitch plane, between the velocity vector and the model center line, independent of roll angle Φ)

β angle of sideslip of balance axis, deg

[redacted]

δ_a control surface aileron angle in body axis system, $\frac{1}{4}[(\delta_2 - \delta_4) + (\delta_3 - \delta_1)]$, deg

δ_n angle of control surface deflection, deg

δ_p control surface pitch angle in body axis system, $\frac{1}{2}(\delta_2 + \delta_4)$, deg

δ_T control surface total angle in balance axis system, $\delta_p \cos \Phi - \delta_y \sin \Phi$, deg

δ_y control surface yaw angle in body axis system, $\frac{1}{2}(\delta_1 + \delta_3)$, deg

Φ angle of roll of model about its longitudinal axis, deg (positive when model, viewed from rear, is rotated clockwise; $\Phi = 0^\circ$ when control surface number 1 is in the positive balance normal-force direction)

A antennas

B body

E control surfaces

H hooks

U umbilical plug

W wing

Subscript

n control surface number 1, 2, 3, or 4, corresponding to top, right, bottom, or left control surface, respectively, when viewed from the rear with $\Phi = 0^\circ$

MODEL AND APPARATUS

The 0.5-scale model, furnished by Hughes Aircraft Company, consisted of a missile having a set of low-aspect-ratio cruciform wings and trailing control surfaces. Photographs of various configurations tested and of the detail of the control surface are presented in figure 2. Protuberances included a set of antennas, hooks, and an umbilical plug. A sketch of the model is shown in figure 3. The arrangement was such that the model could be rotated about its longitudinal axis (or about the balance axis) through a range of roll angles from -135° to 45° and each control surface could be deflected from -35° to 35°. In order to facilitate the investigation, these changes in roll angles and control surface deflections

were remotely controlled. The force measuring device was a six-component, internal-type, strain-gage balance. Since the estimated rolling moments were small in comparison to the capacity of the balance rolling-moment gage, these measurements were obtained from a special strain-gage assembly mounted on the forward end of the balance. Hinge moments were measured by strain gages on each of the four control surface supports.

PROCEDURE

Stability data with neutral control surface position were obtained throughout an angle-of-attack range of -5° to 25° at $\beta \approx 0.25^\circ$ (or essentially 0). The Mach numbers were 1.60, 2.00, and 2.30 and the Reynolds number was approximately 0.6×10^6 based on a reference diameter of 3.2 inches. For the complete configuration (BWEHU) the model was rolled through a range of angles from -135° to 45°. For configuration BWE only three roll angles were investigated: 0°, 22.5°, and 45°. Configurations BW and BWEA were investigated at roll angles of 0° and 45°.

Control surface effectiveness was obtained for configuration BWE only. At angles of attack from 0° to 25° pitch deflection δ_p was varied from -35° to 15° and yaw deflection was set equal to $-\delta_p \tan \Phi$.

The effect of control surface aileron angle (δ_a) on the trim condition was obtained for configuration BWE. For these tests, aileron angles from 0° to 5° were superposed on trim values of total deflection δ_T. These trim values were selected for each α, Φ, and M from the previously obtained stability data.

PRESENTATION OF DATA

The data presented for the various configurations, and the corresponding figure numbers, are tabulated below.

Configuration	X axis	Y axis	M	Φ, deg	Figure
B	α	C_N, C_m, C_A	1.6, 2.0, 2.3	0	4
BW	α	C_N, C_m, C_A, C_l	↓	0, 45	5
BWE	α	$C_N, C_m, C_A, C_l, C_n, C_Y, Ch_n$	↓	0, 22.5, 45	6
BWEA	α	C_N, C_m, C_A, C_l	↓	0, 45	7
BWEHU	α	C_N, C_m, C_A, C_l, Ch_n	↓	-135 to 45	8
BWE	δ_T	C_N, C_m, C_A, C_l, C_n	↓	0, 22.5, 45	9-13
BWE	$\delta_{2,4}$	Ch_2, Ch_4	↓	0, 45	14
BWE	δ_n	Ch_n	↓	22.5	15
BWE	δ_a	C_l	↓	0, 22.5, 45	16
BWE	δ_a	C_m	↓	0, 22.5, 45	17

Hinge-moment characteristics with control surfaces undeflected are included where applicable. Only a limited amount of C_Y and C_n data is presented in this report, since these coefficients generally are negligible and of secondary importance. The apparent shift in C_N and C_m at zero angle of attack at $M = 1.60$ as indicated in figures 8(a) and 8(b) is probably due to a zero drift in the balance normal-force gage. The data of figure 17 were obtained with aileron deflections superposed on trim values of δ_T. Trim values of δ_T for each value of α, Φ, and M were selected from figure 10.

Ames Research Center
National Aeronautics and Space Administration
Moffett Field, Calif., Apr. 10, 1959

REFERENCES

1. Reed, Verlin D., and Wilson, Warren S.: Static Stability and Control Characteristics of a 0.5-Scale Model of the Hughes GAR-11 Missile at Mach Numbers From 0.8 to 1.4 (COORD. NO. AF-AM-162). NASA MEMO 6-8-59A, 1959.

2. Frank, Joseph L., and Kauffman, Ronald C.: Static Stability and Control Characteristics of a 0.5-Scale Model of the Hughes GAR-11 Missile at Mach Numbers From 2.5 to 3.5 (COORD. NO. AF-AM-162). NASA MEMO 6-7-59A, 1959.

3. Bluestein, T.: Test of a 0.11-Scale Model 52 Missile in the J. P. L. 12-Inch Supersonic Wind Tunnel. Hughes Aircraft Company Wind Tunnel Data Rep. No. 88, Aug. 1958.

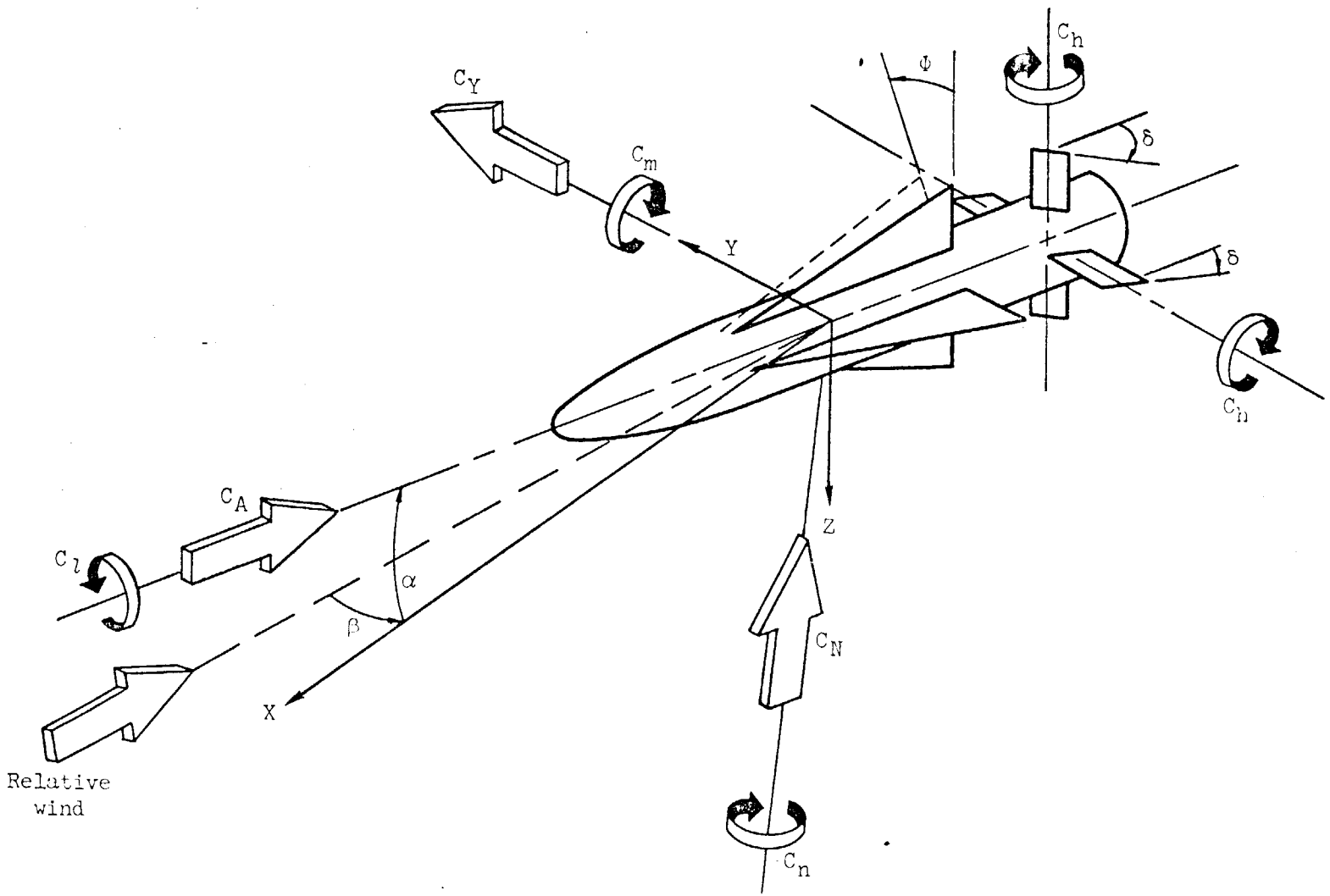

Figure 1.- System of axes and positive direction of forces, moments, and angles.

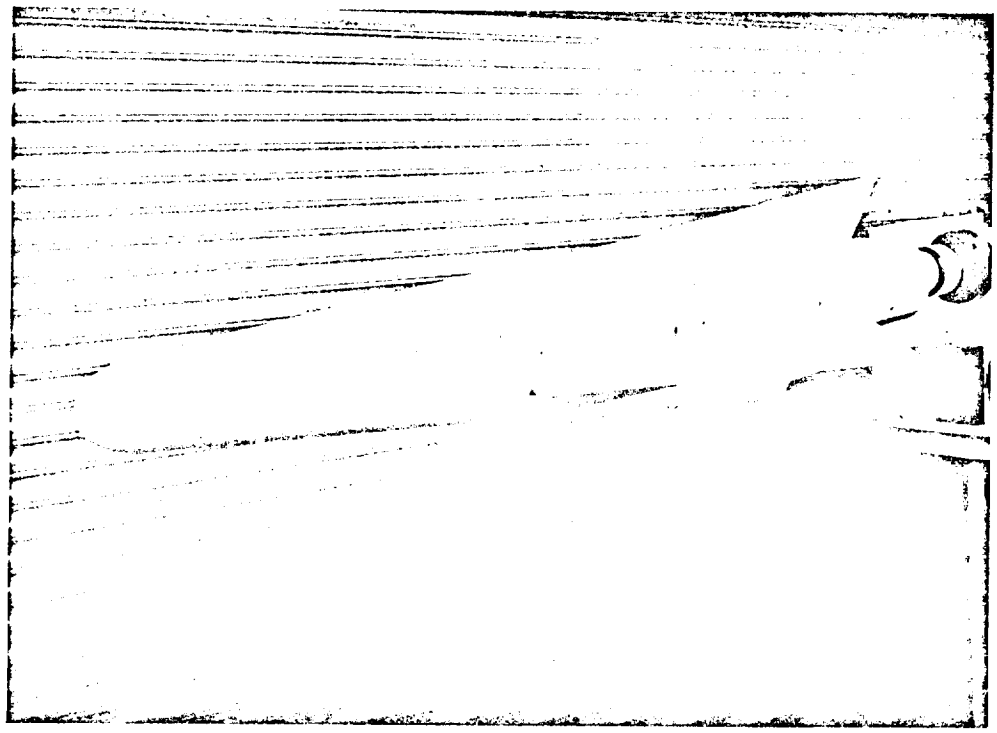

A-23936

(a) Configuration BW.

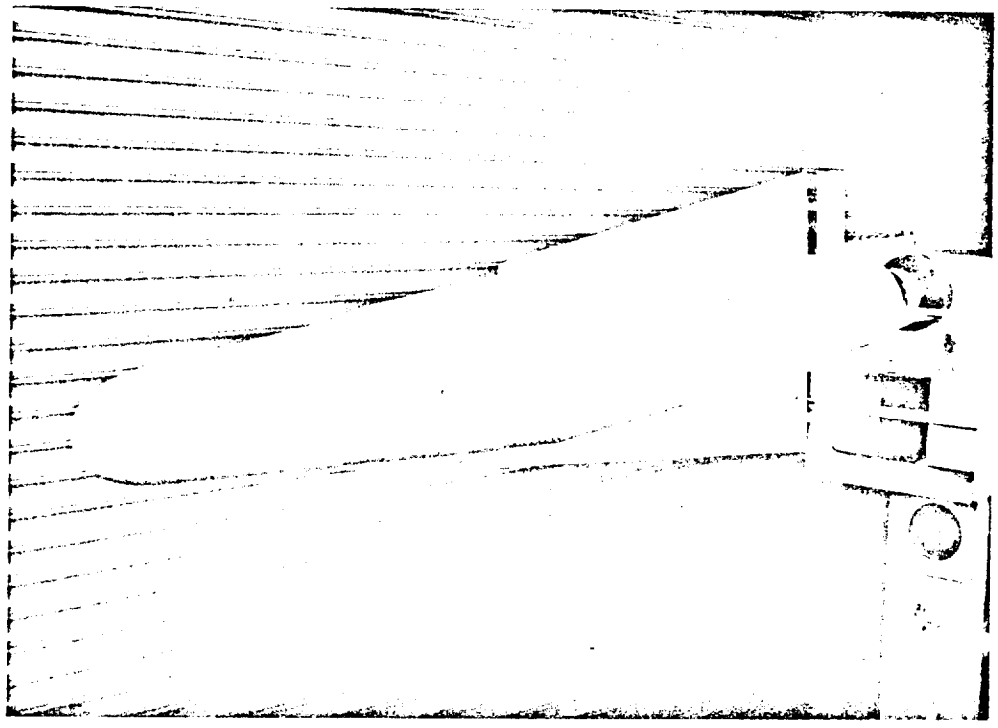

A-23933

(b) Configuration BWEA.

Figure 2.- Photographs of the model.

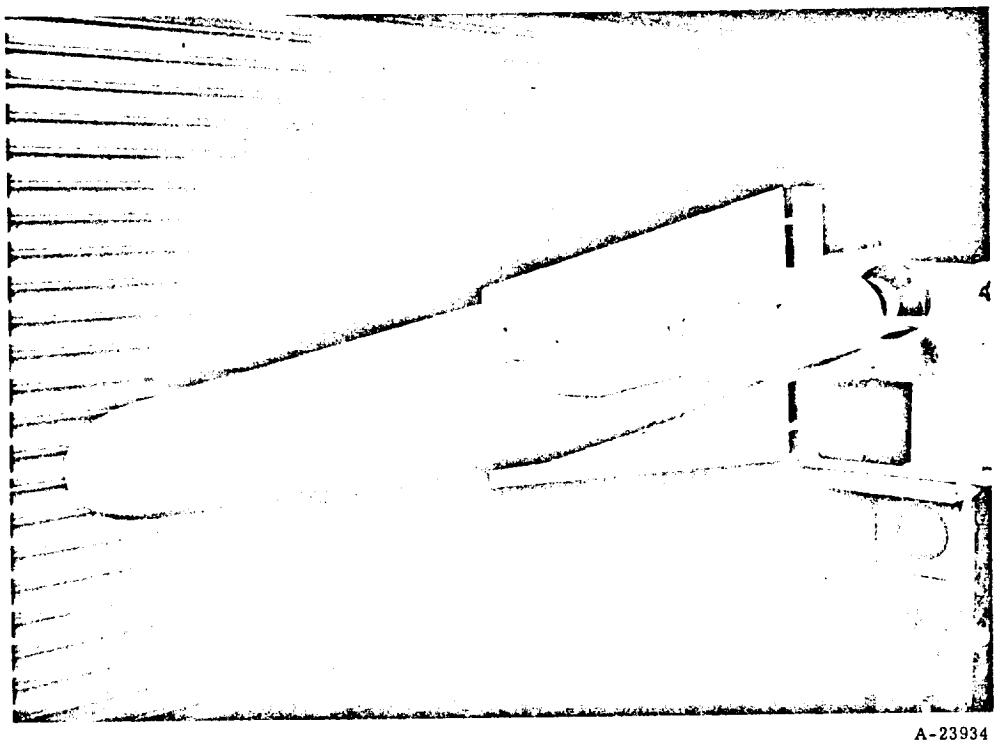

A-23934

(c) Configuration BWEHU.

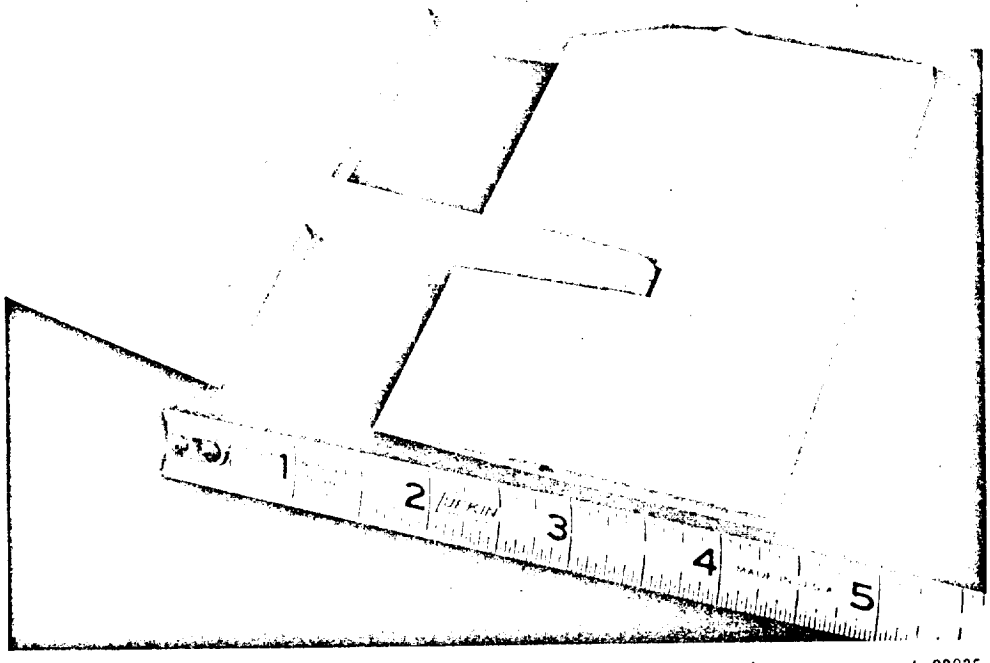

A-23935

(d) Detail of control surface.

Figure 2.- Concluded.

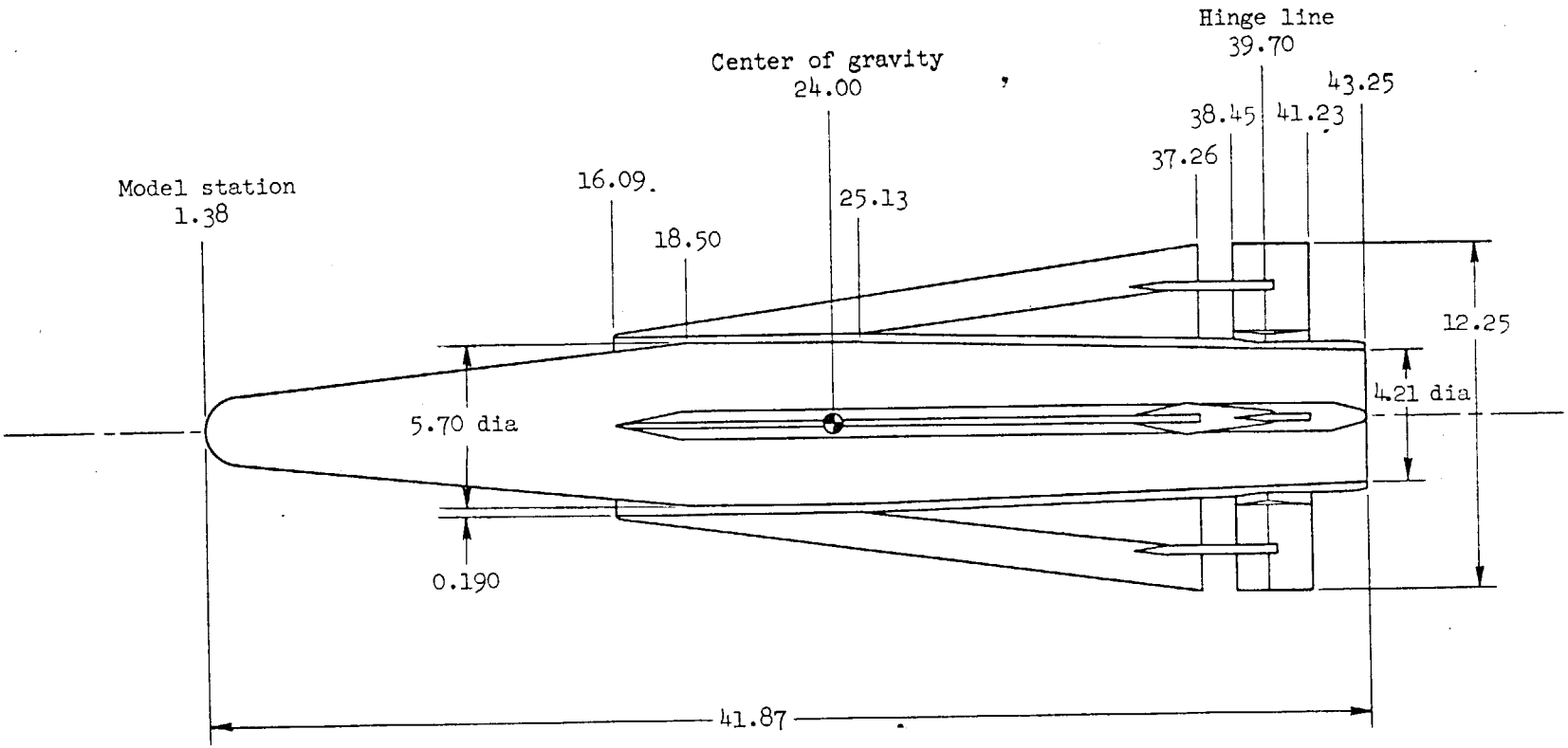

Note: All dimensions and model stations are in inches.

Figure 3.- Sketch of model.

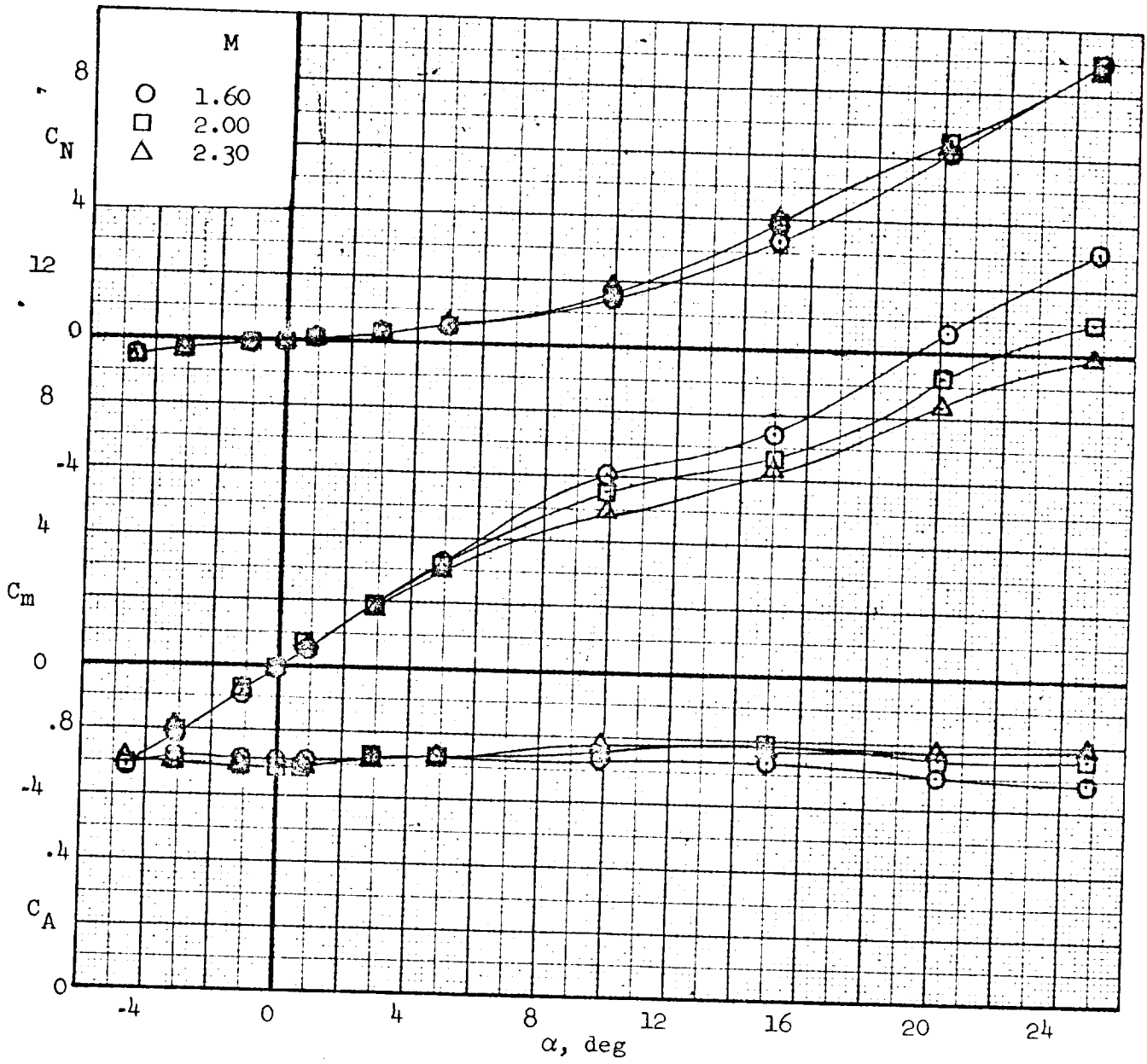

Figure 4.- Aerodynamic characteristics for the B configuration.

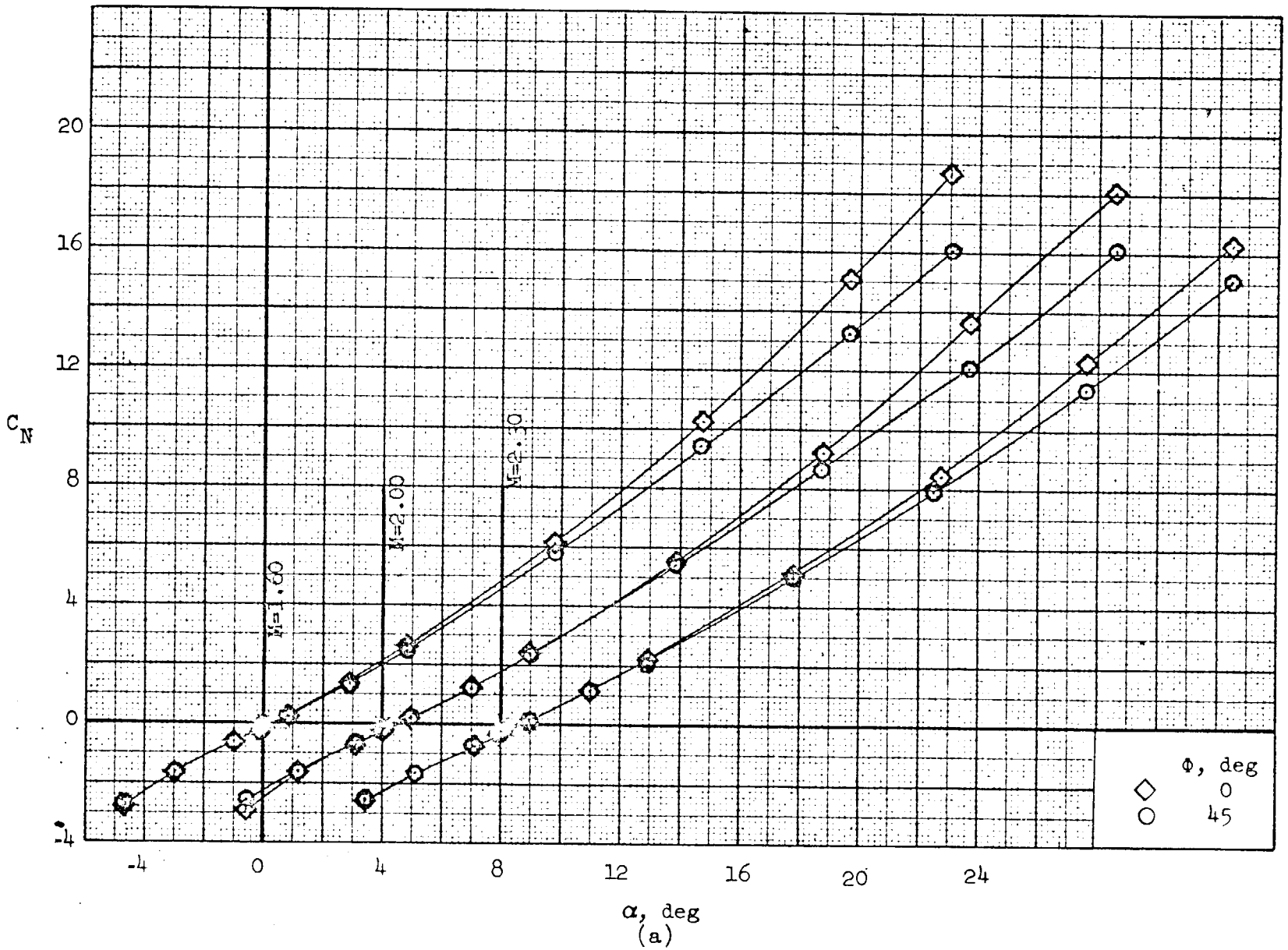

Figure 5.- Aerodynamic characterics for the BW configuration.

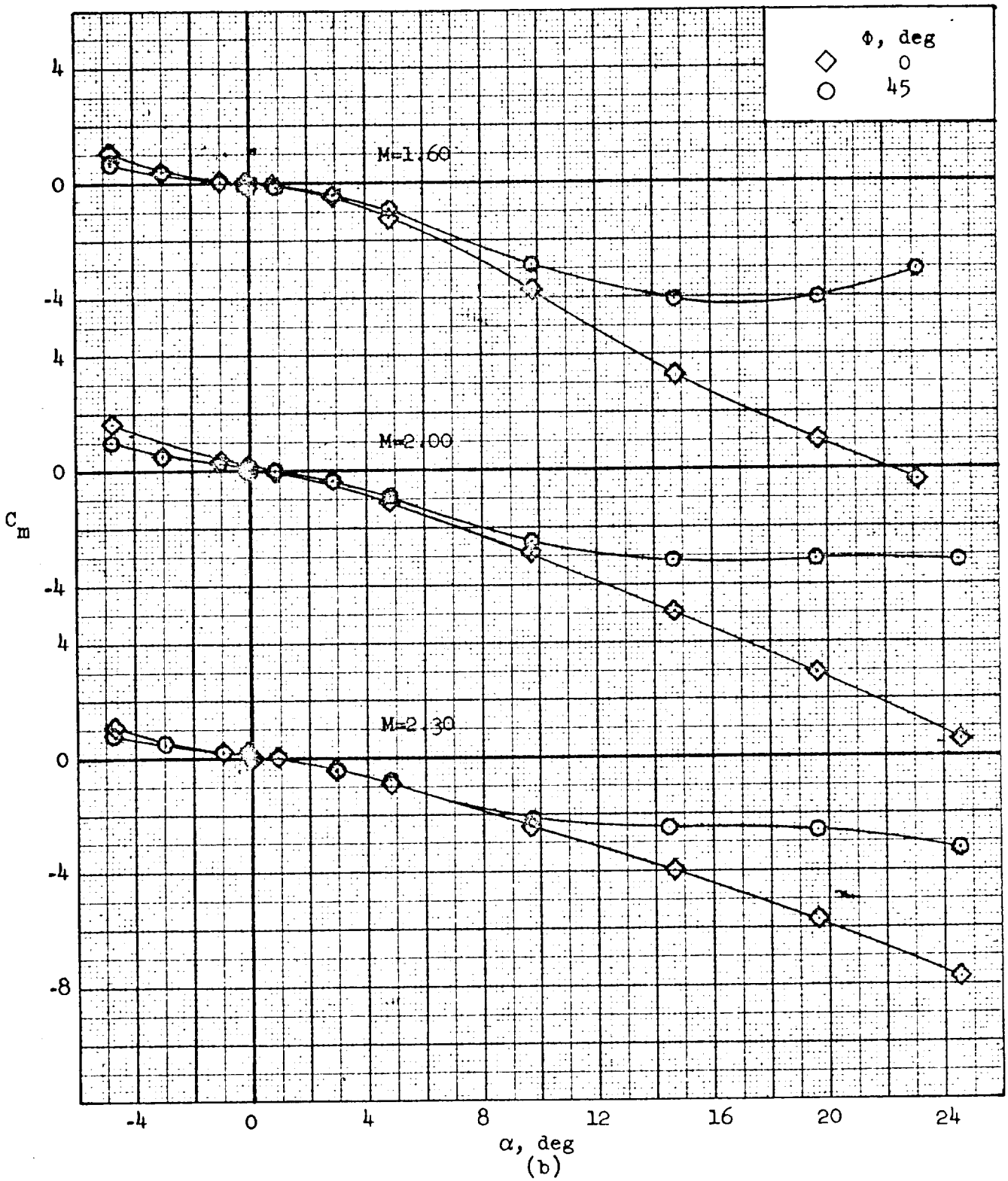

(b)

Figure 5.- Continued.

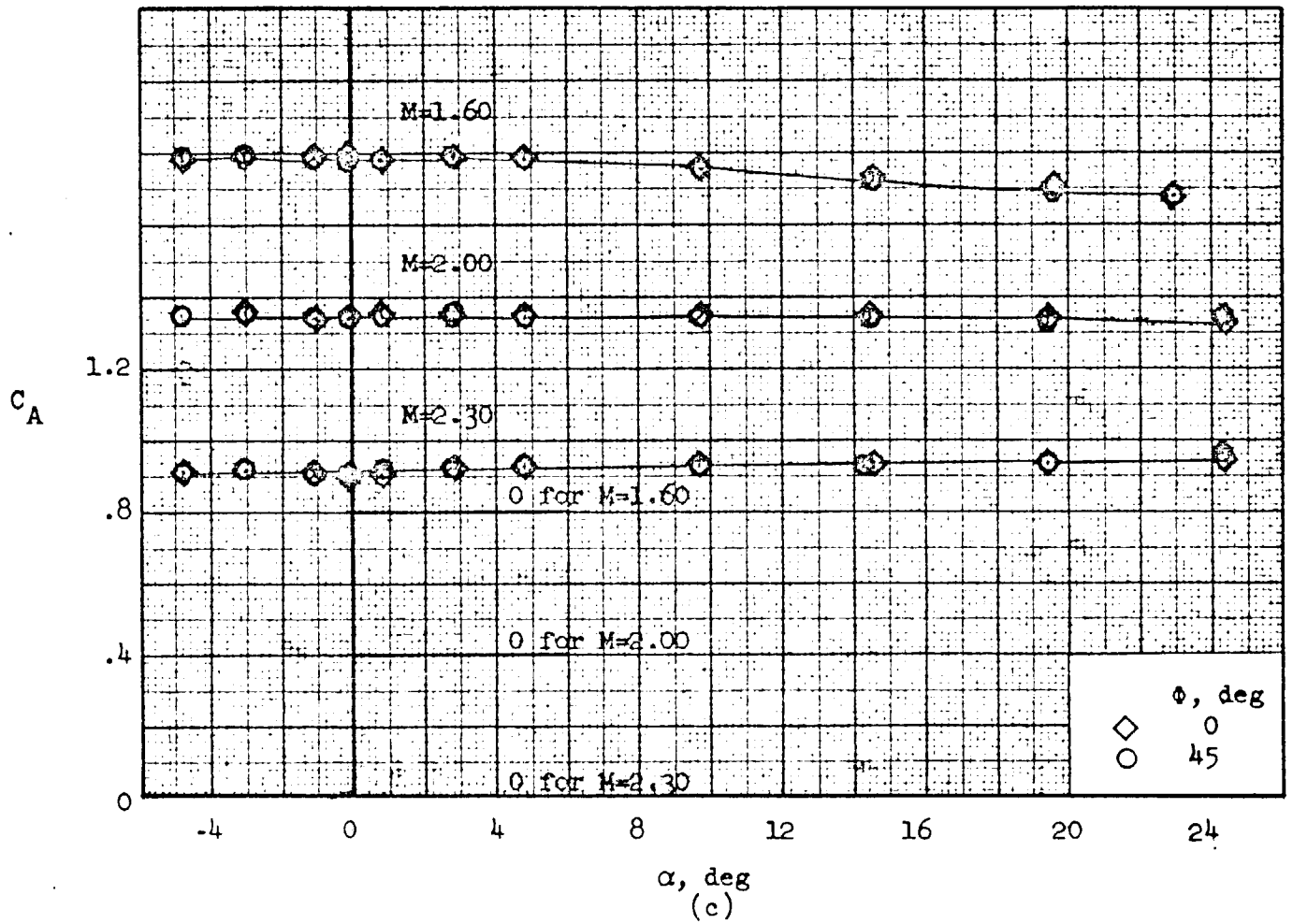

(c)

Figure 5.- Continued.

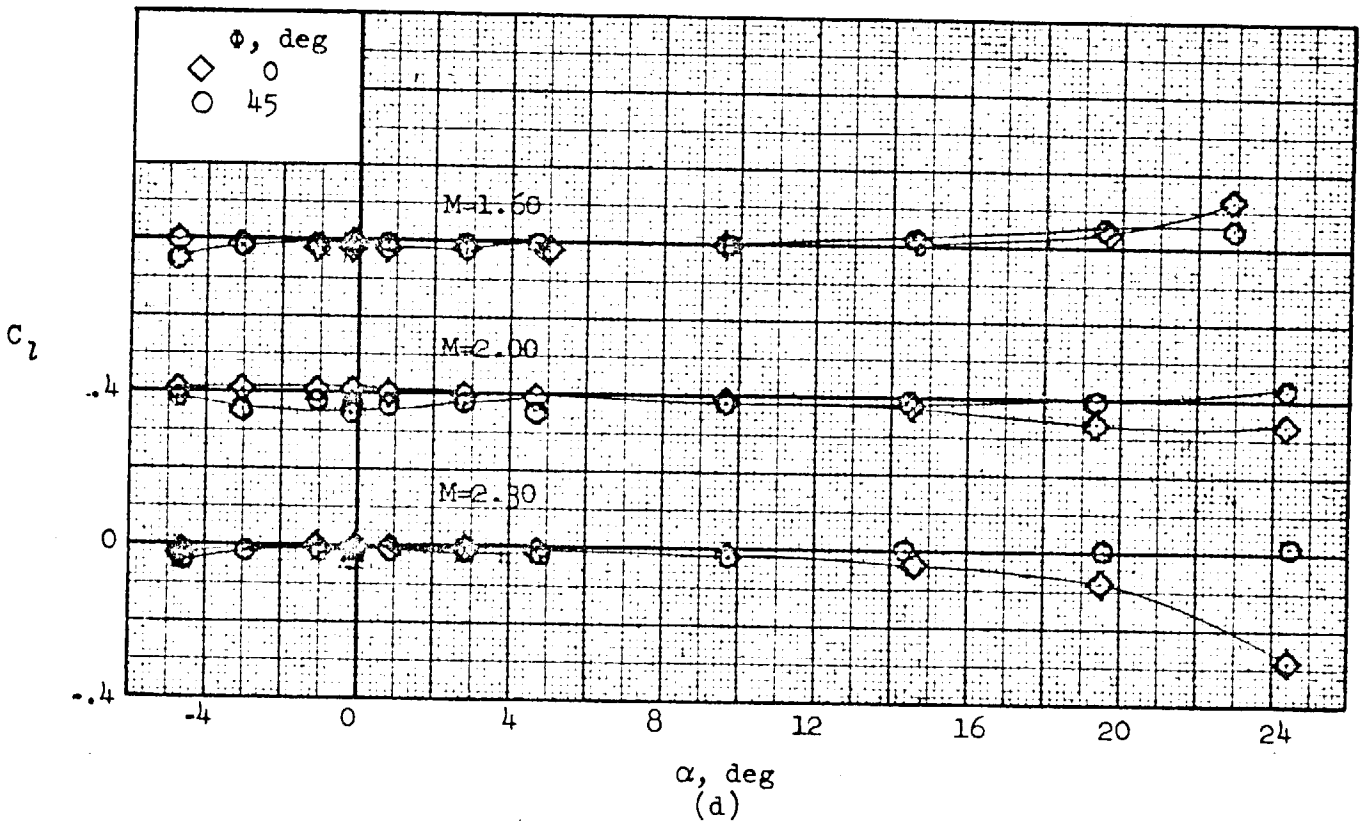

(d)

Figure 5.- Concluded.

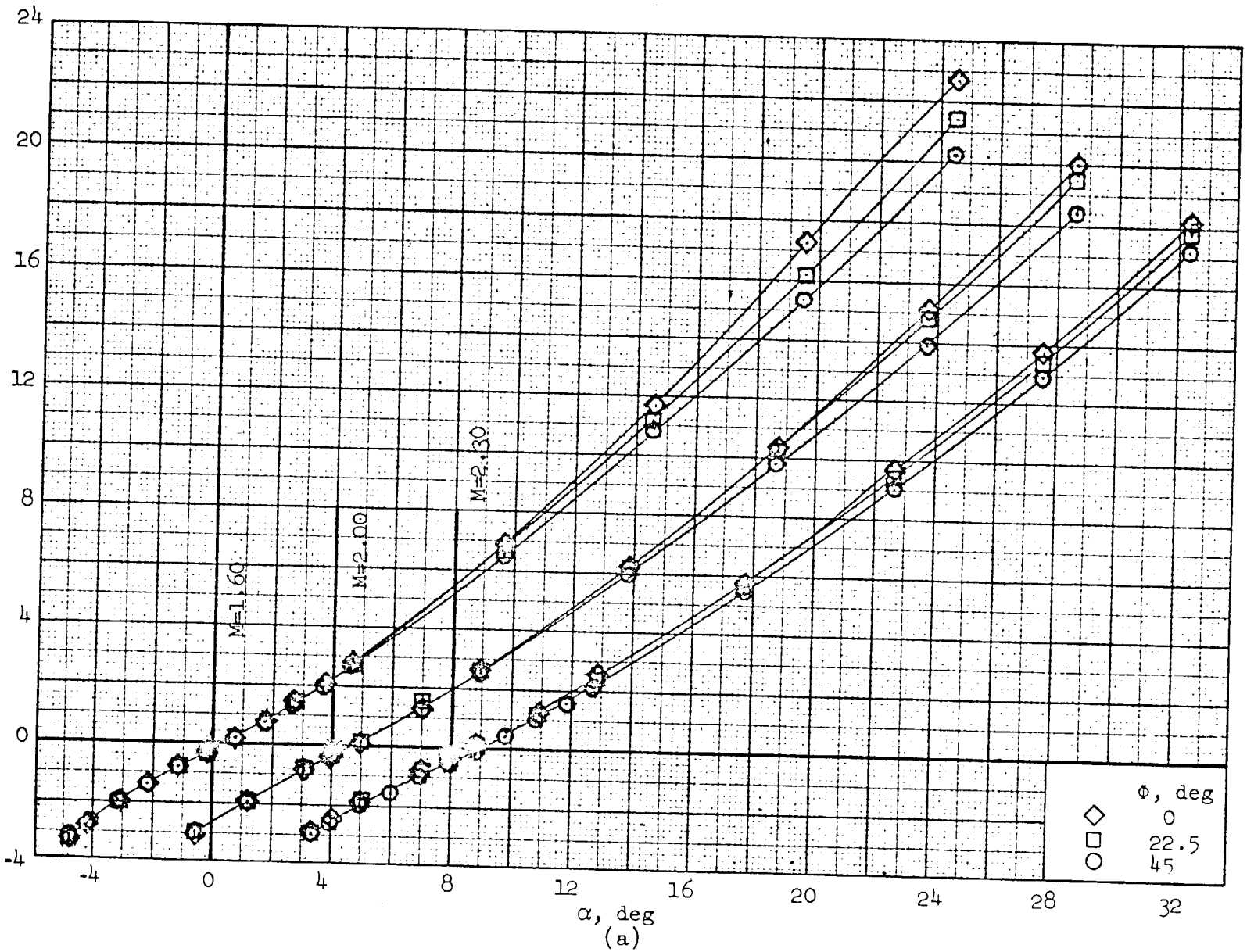

(a)

Figure 6.- Aerodynamic characteristics for the BWE configuration.

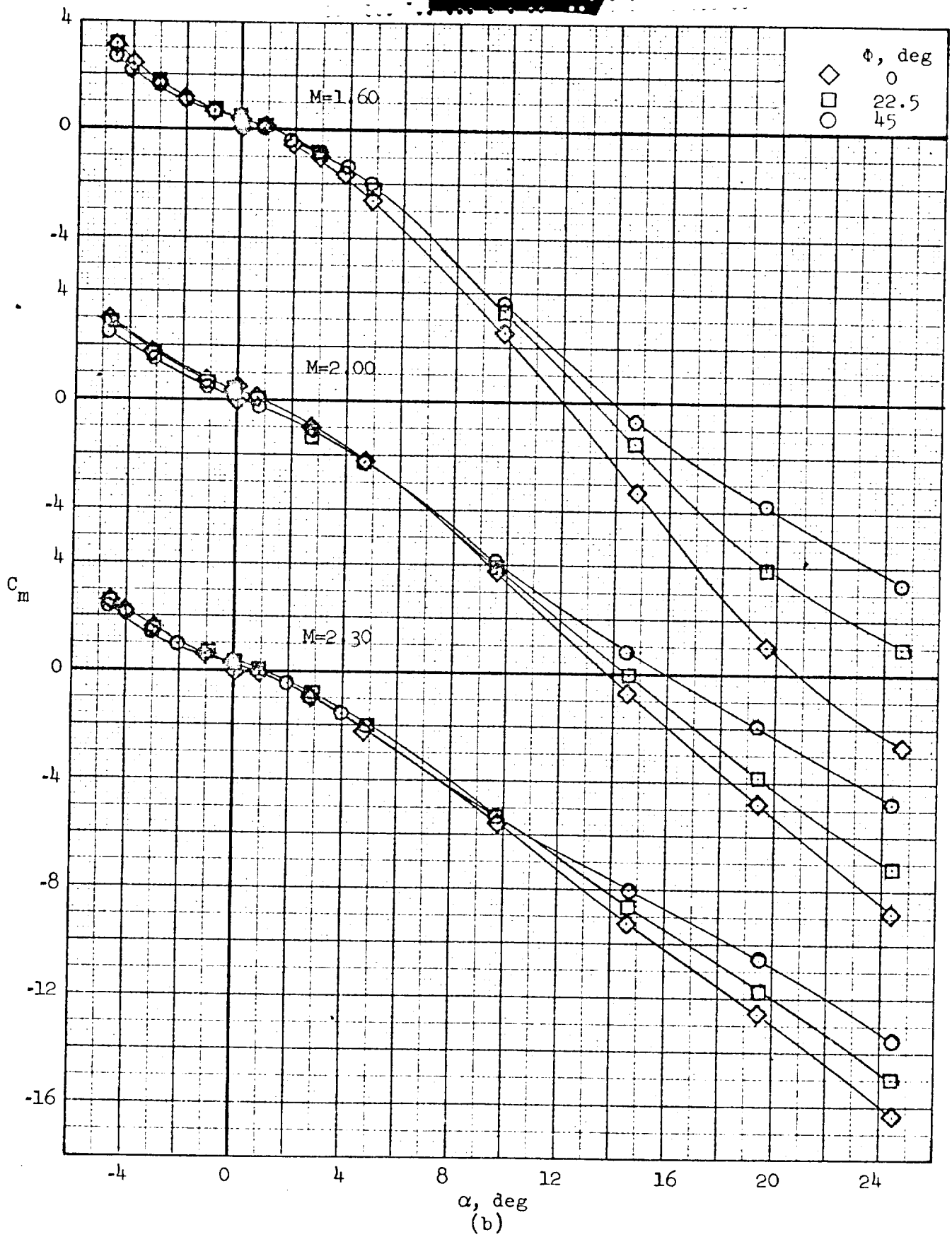

(b)

Figure 6.- Continued.

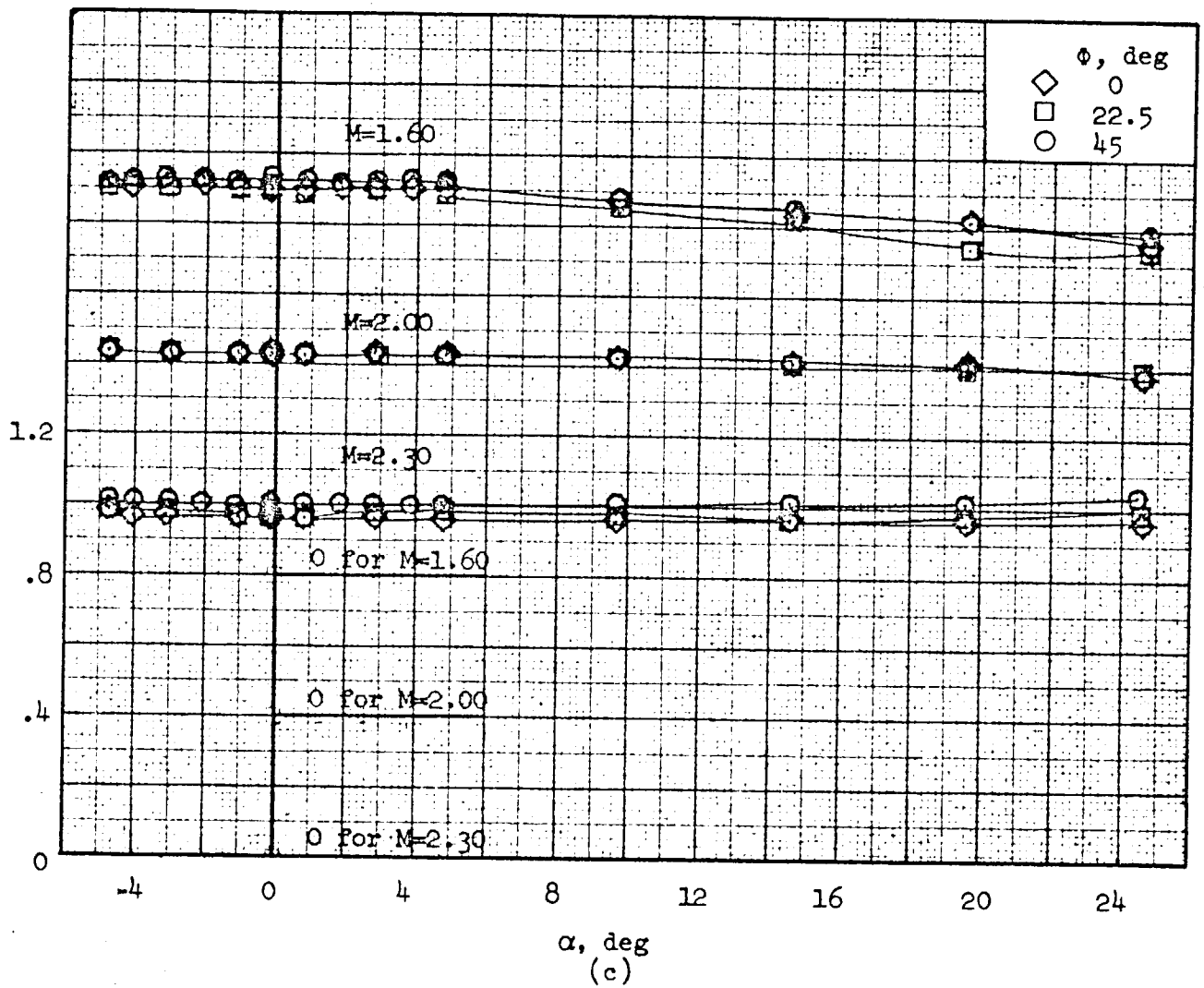

(c)

Figure 6.- Continued.

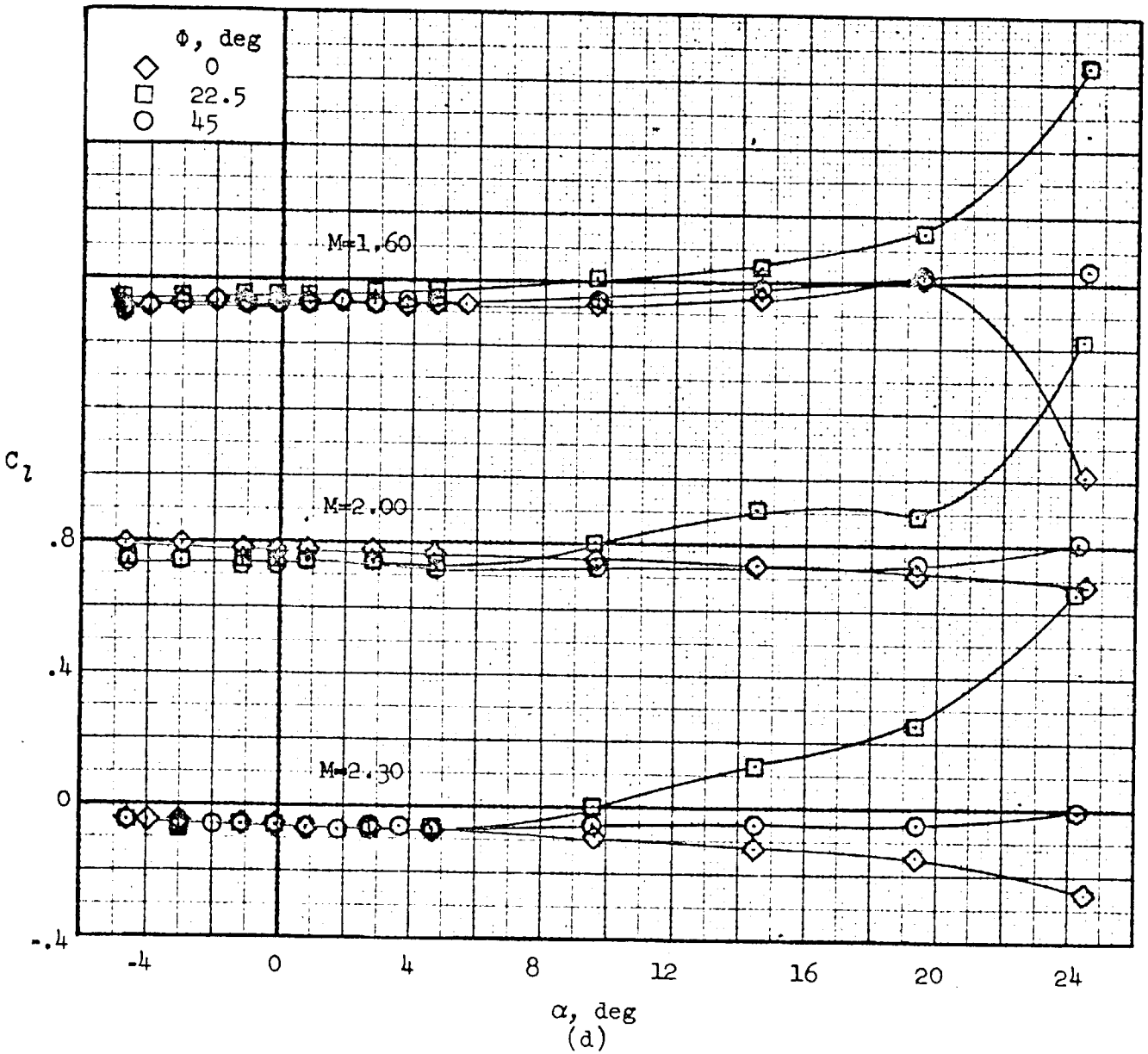

(d)

Figure 6.- Continued.

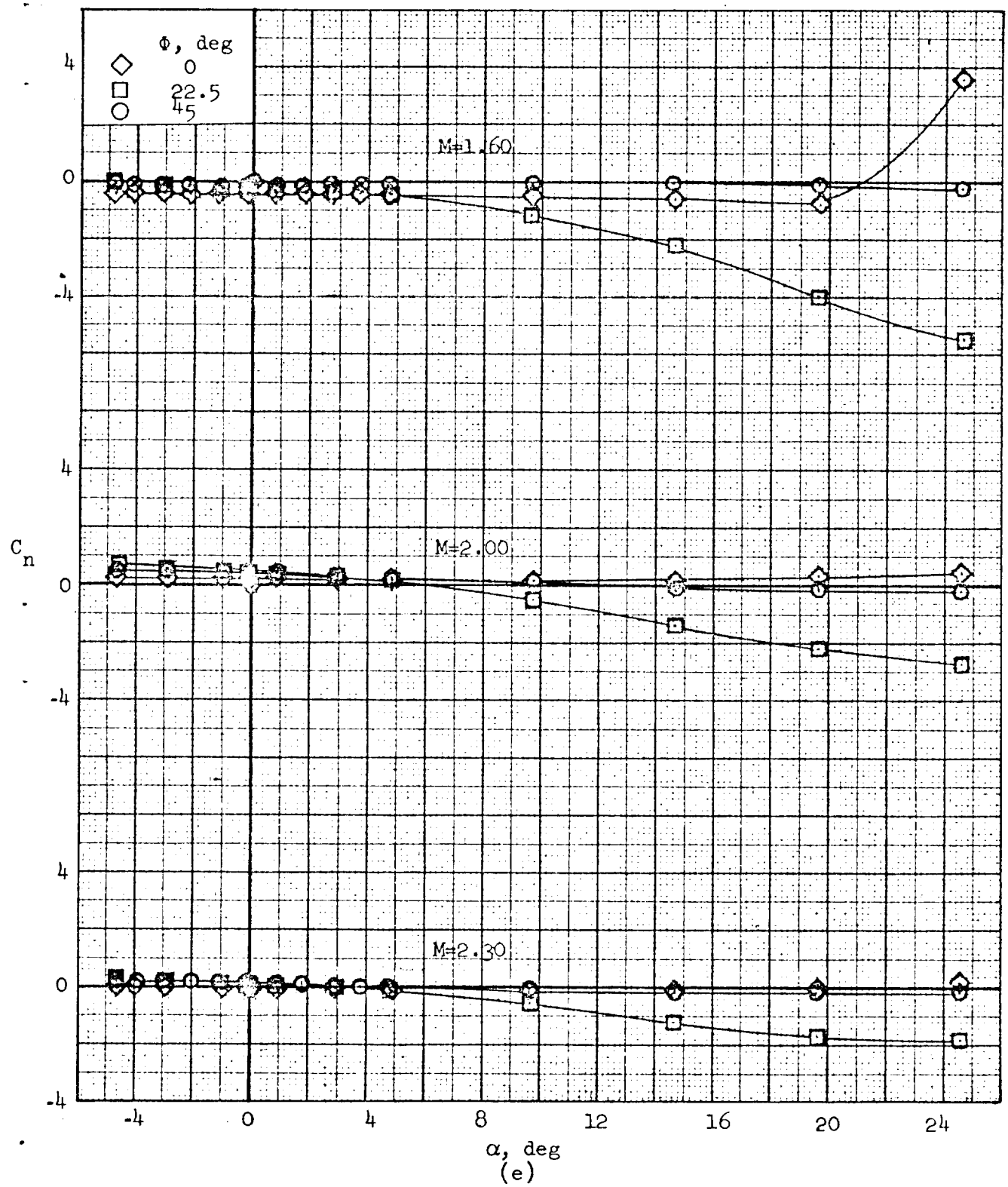

(e)

Figure 6.- Continued.

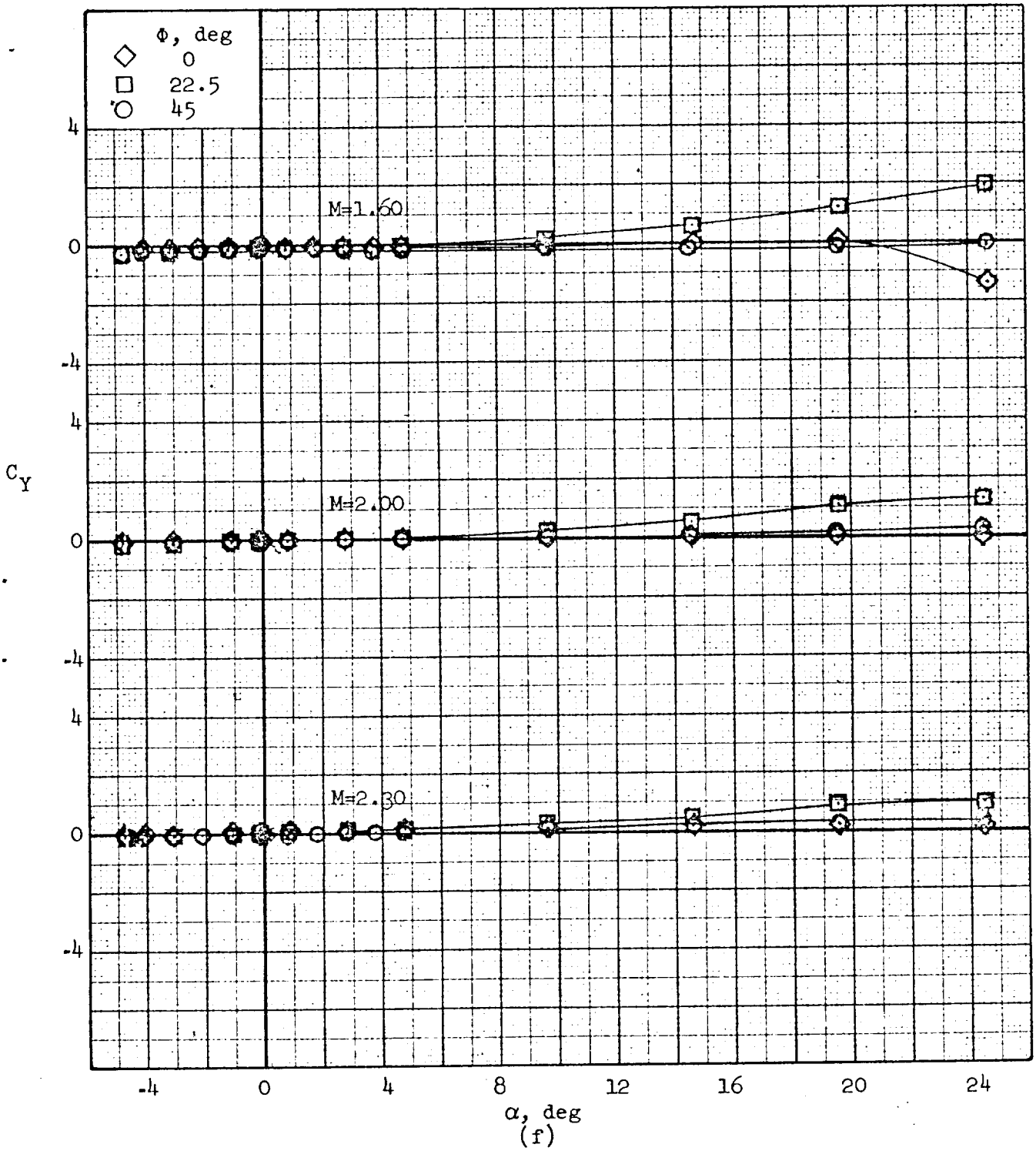

(f)

Figure 6.- Continued.

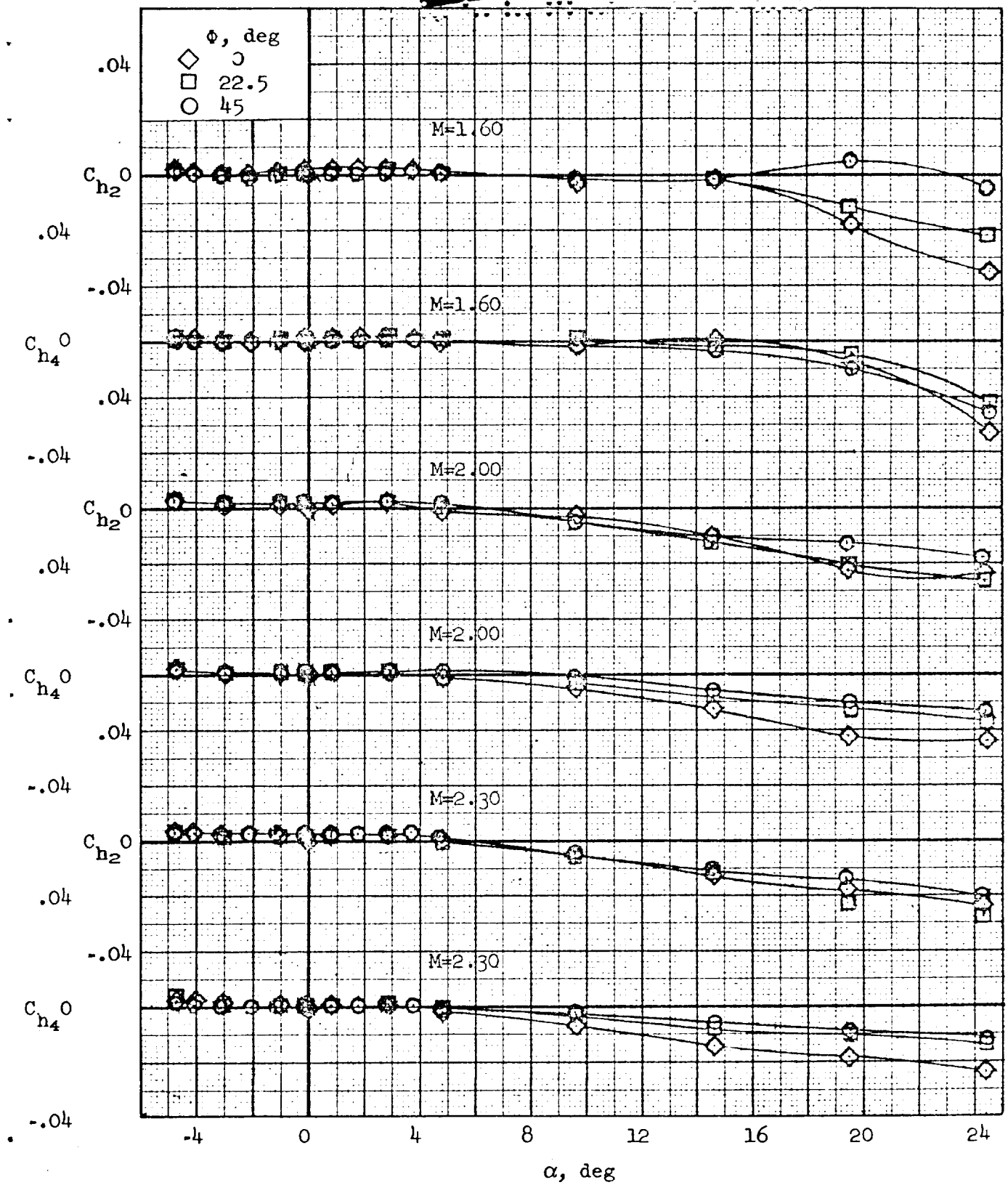

(g)

Figure 6.- Continued.

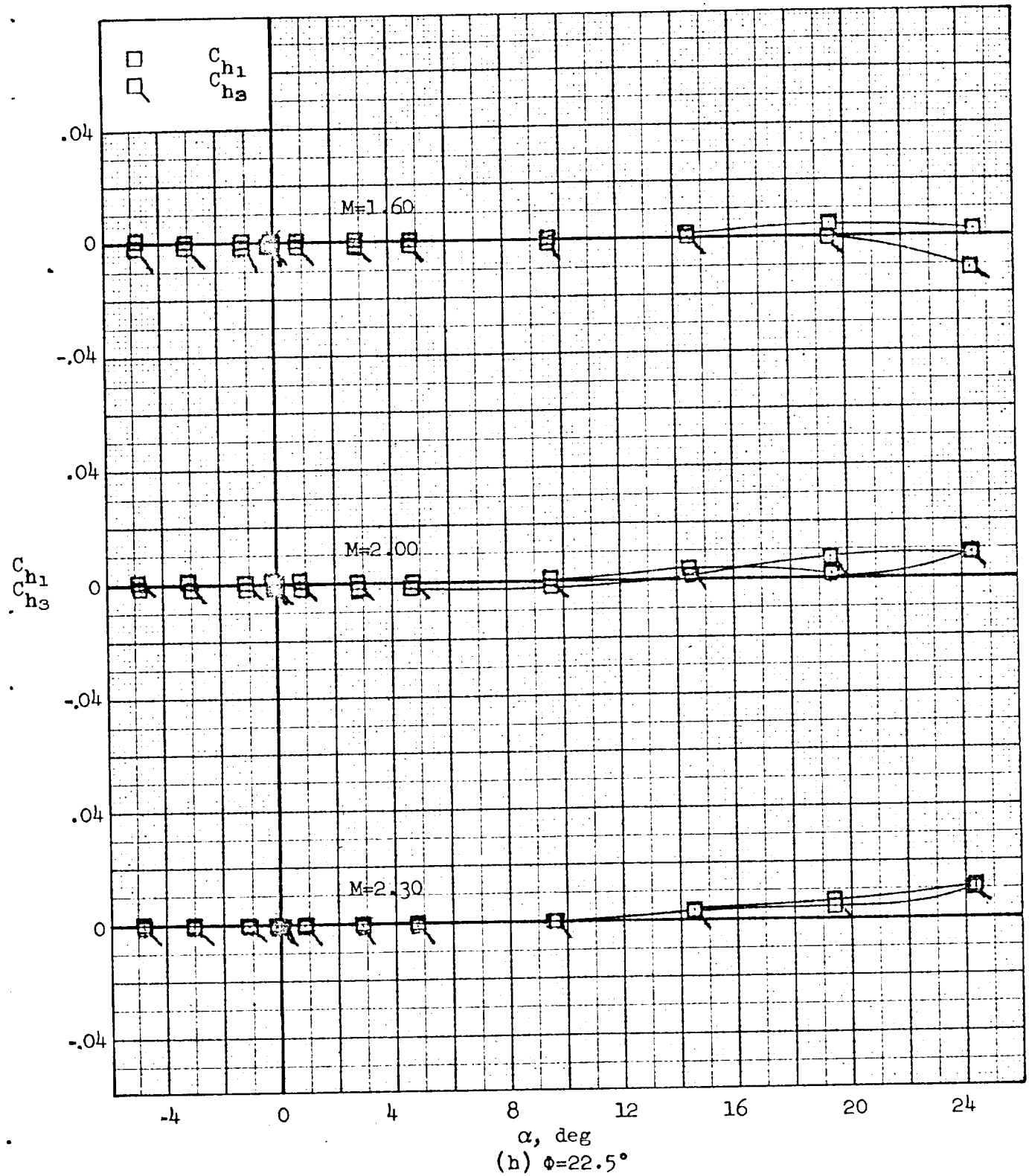

(h) Φ=22.5°

Figure 6.- Concluded.

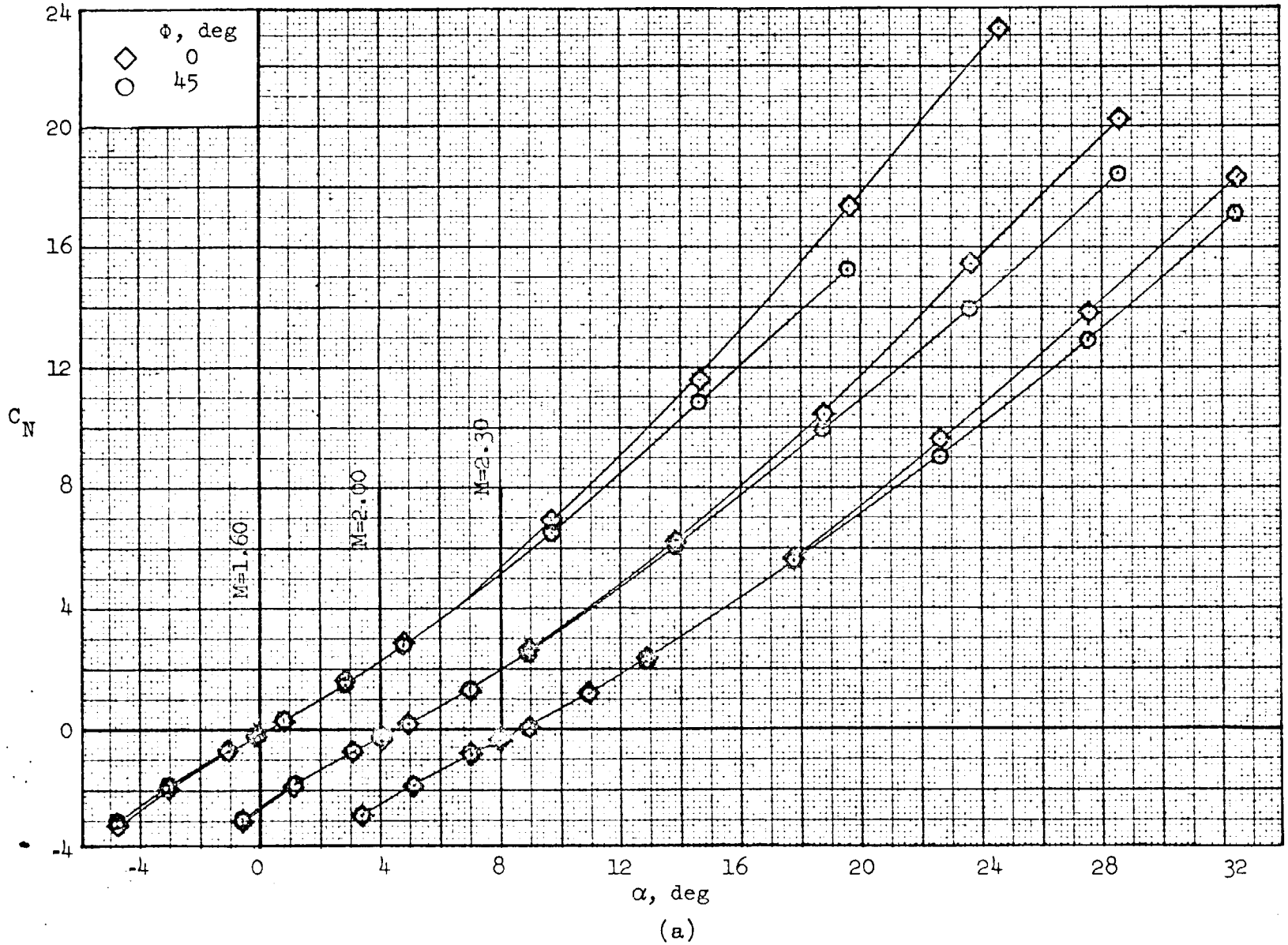

(a)

Figure 7.- Aerodynamic characteristics for the BWEA configuration.

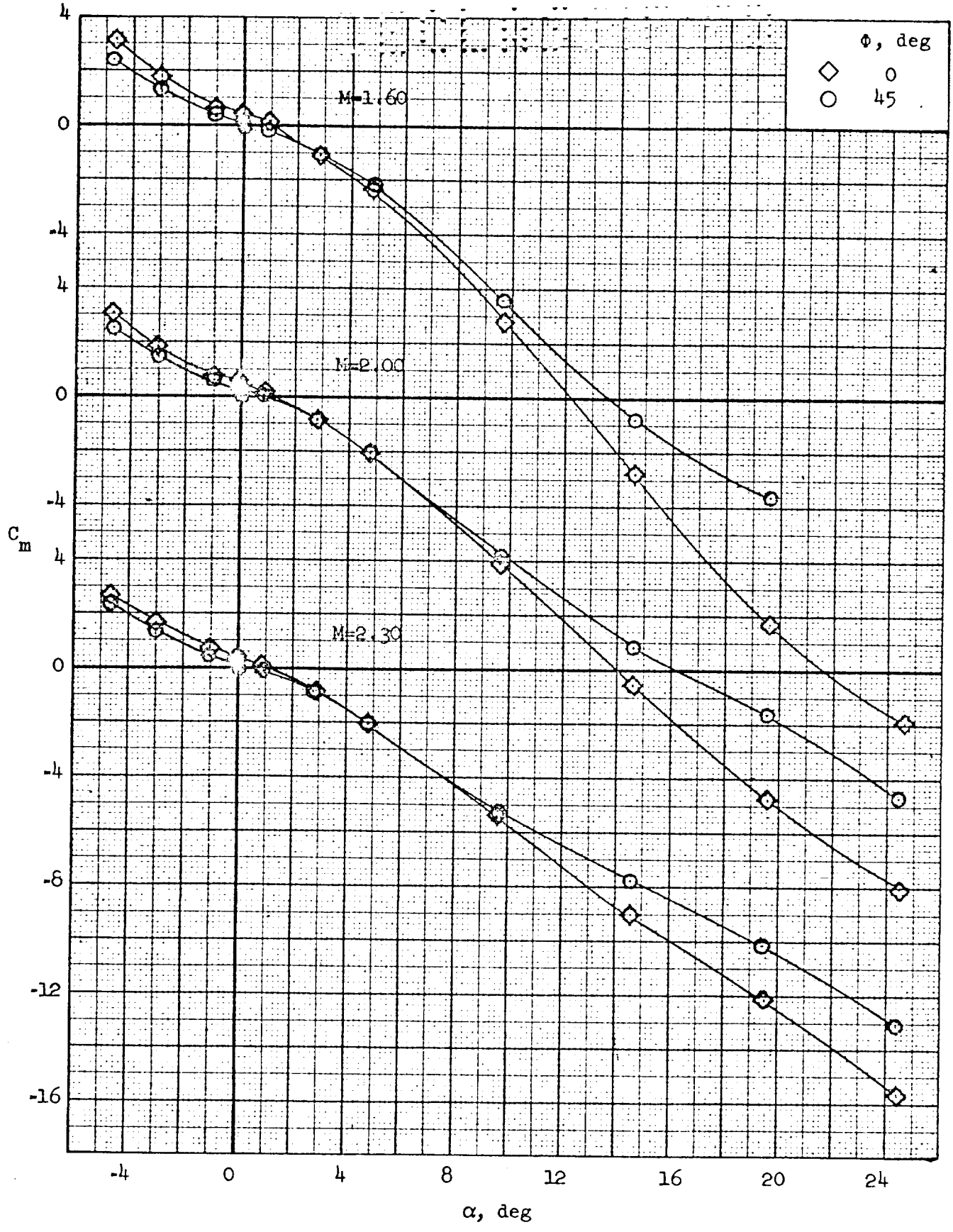

(b)

Figure 7. - Continued.

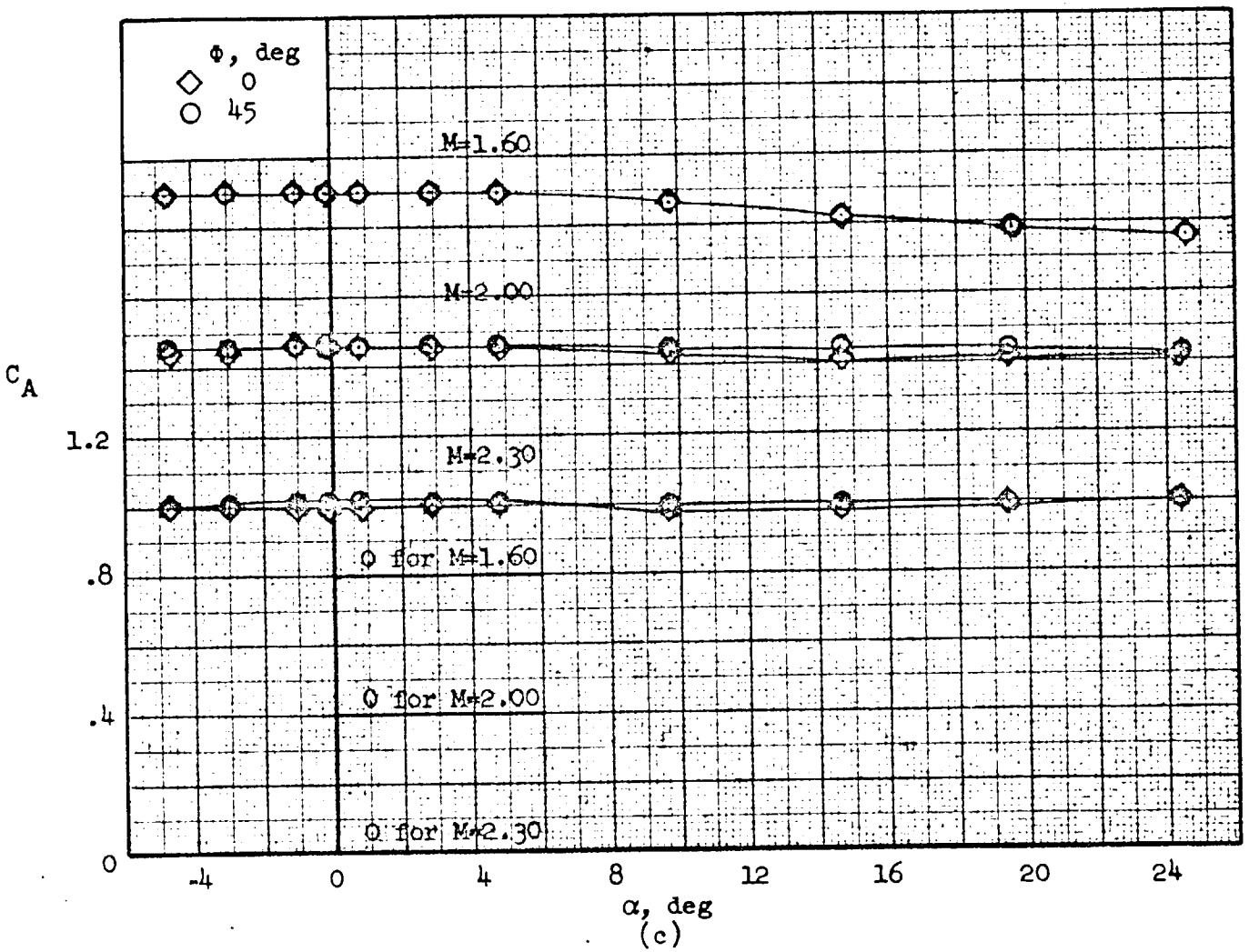

(c)

Figure 7.- Continued.

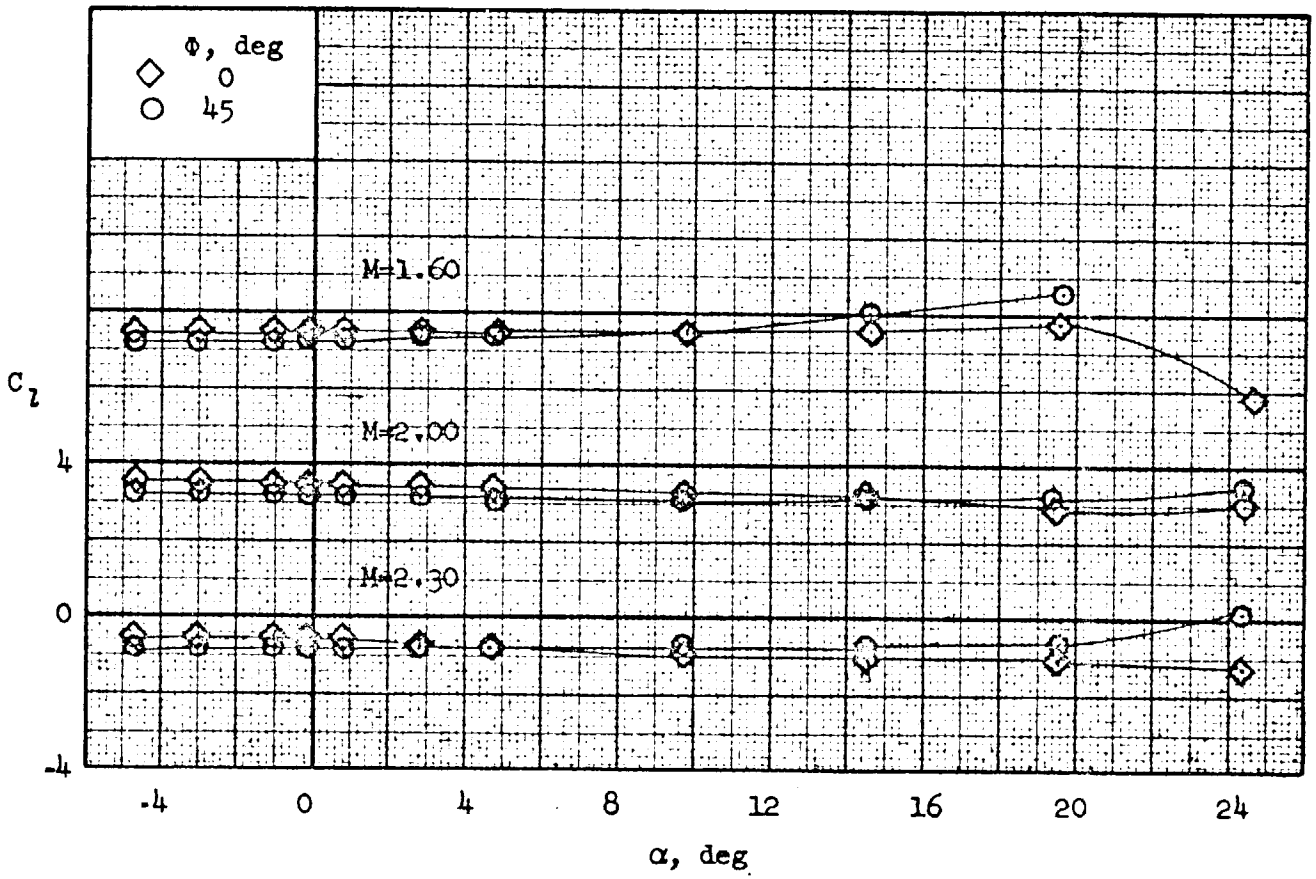

(d)

Figure 7.- Concluded.

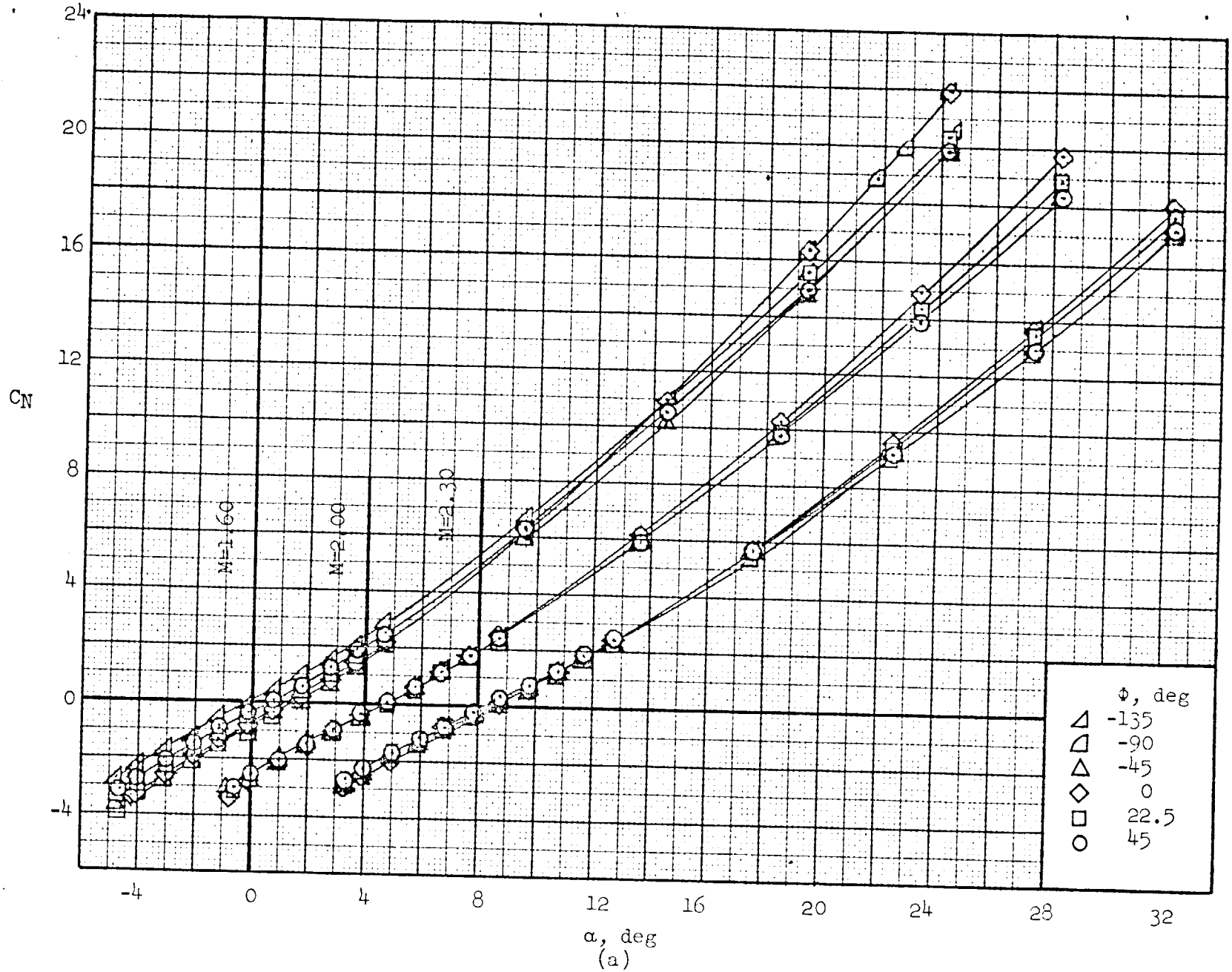

(a)

Figure 8.- Aerodynamic characteristics for the BWEHU configuration.

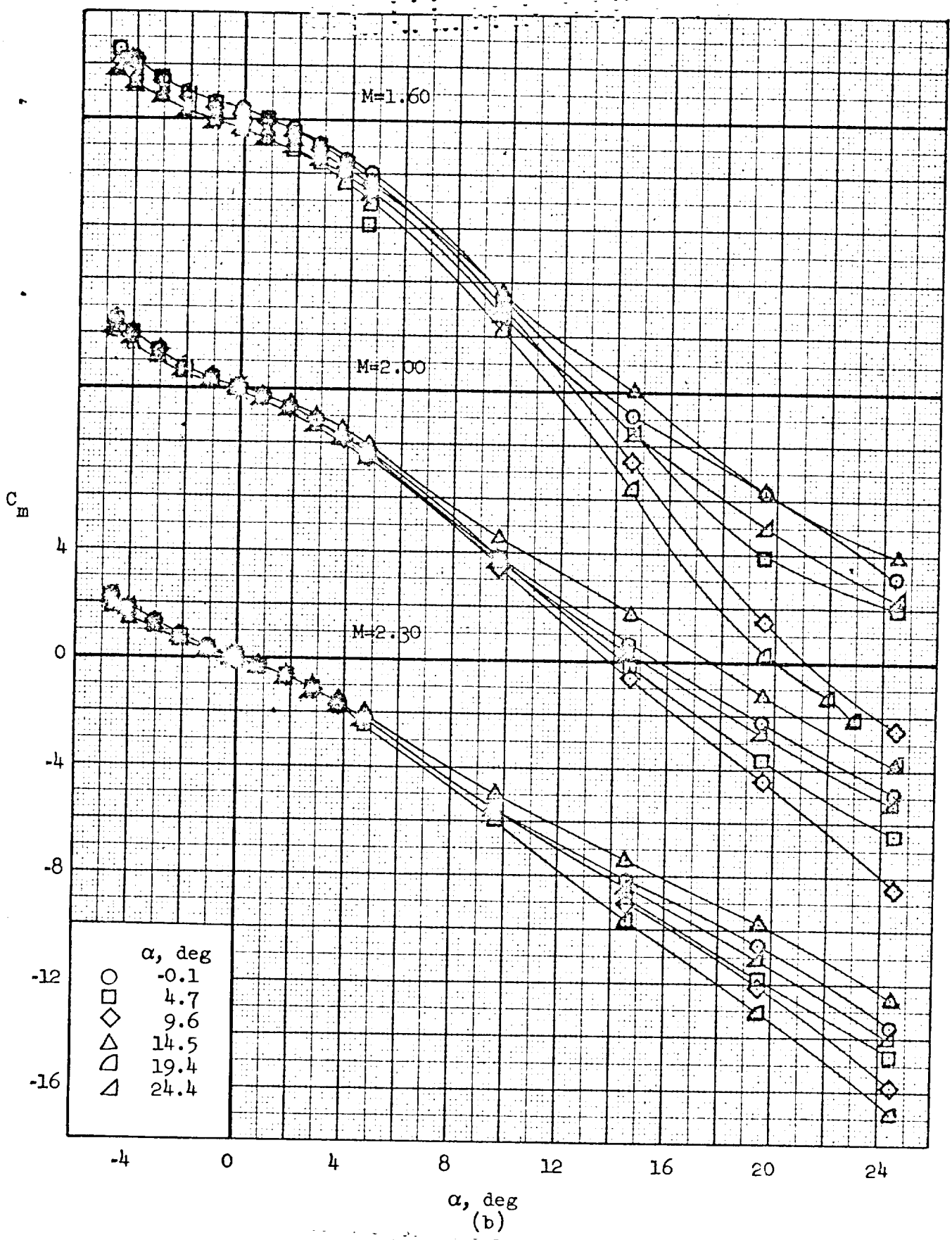

(b)

Figure 8.- Continued.

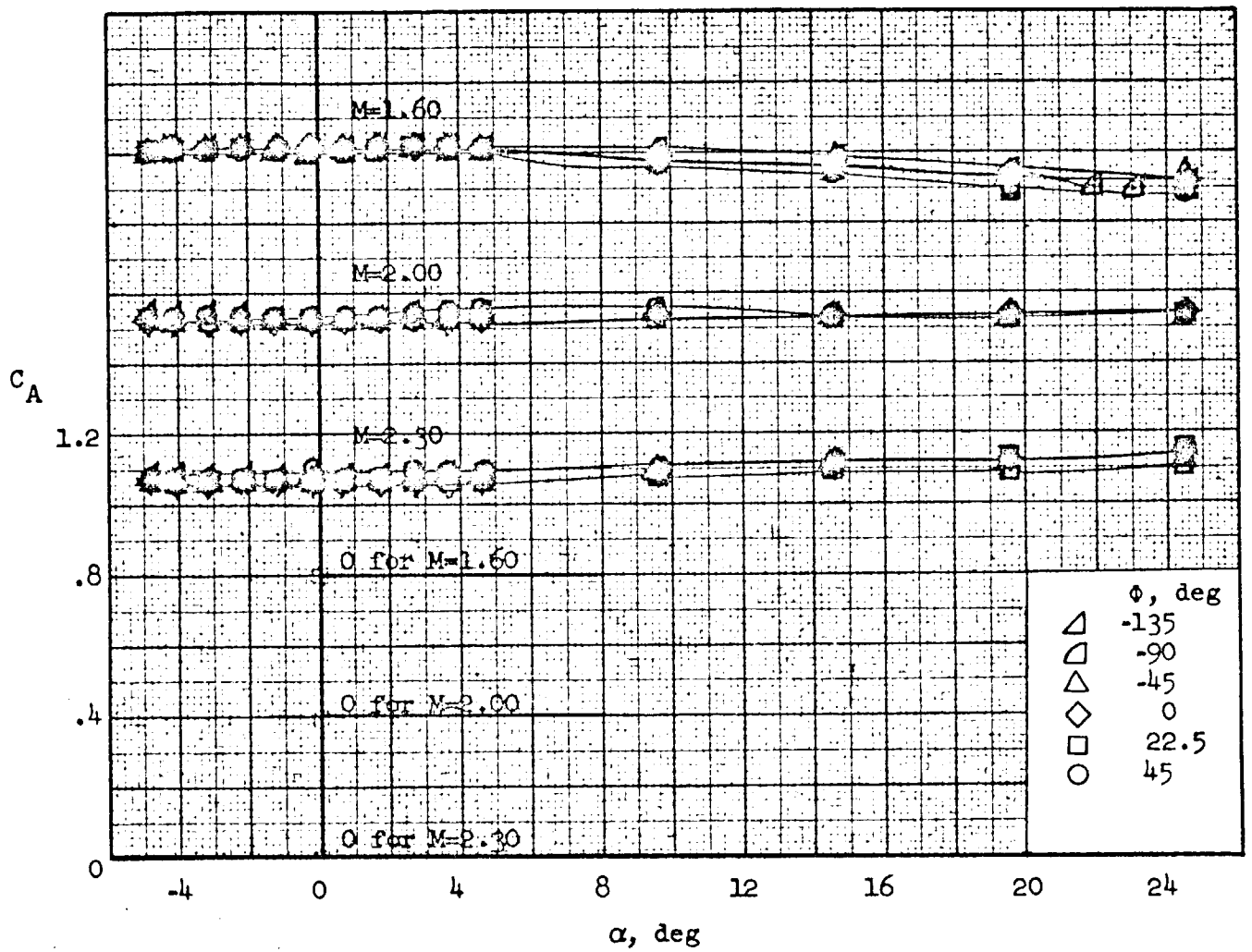

(c)

Figure 8.- Continued.

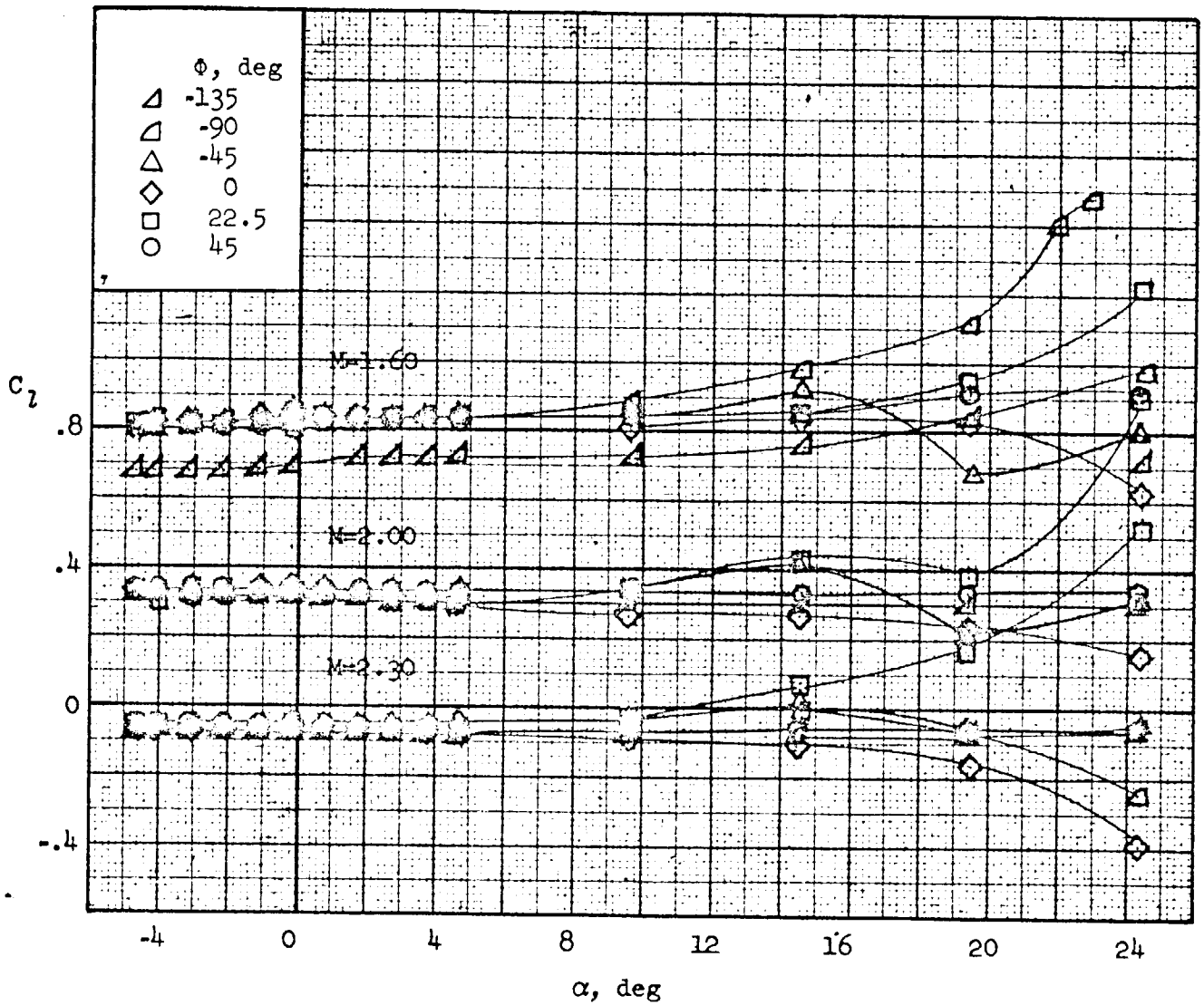

(d)

Figure 8.- Continued.

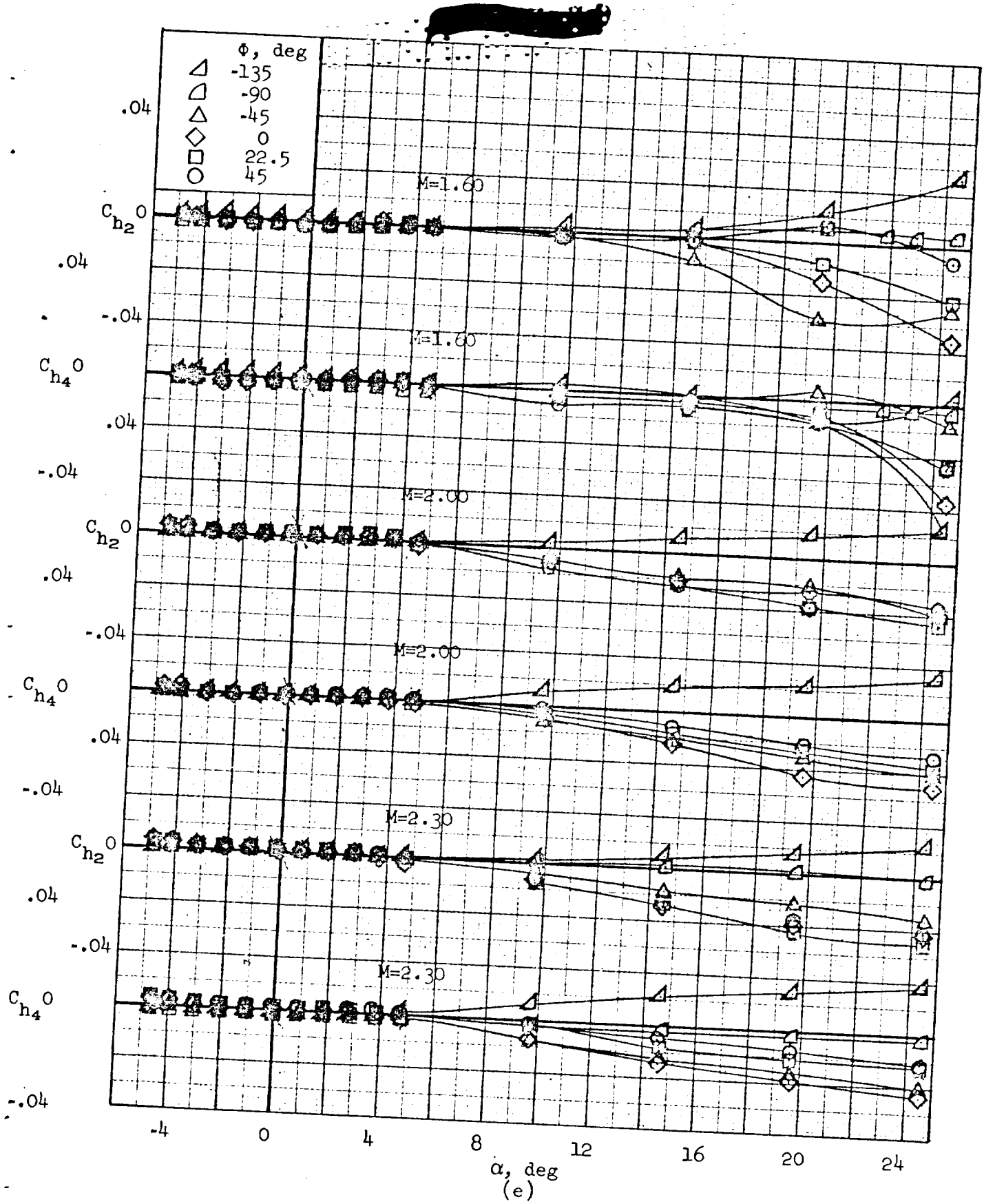

(e)

Figure 8. Continued.

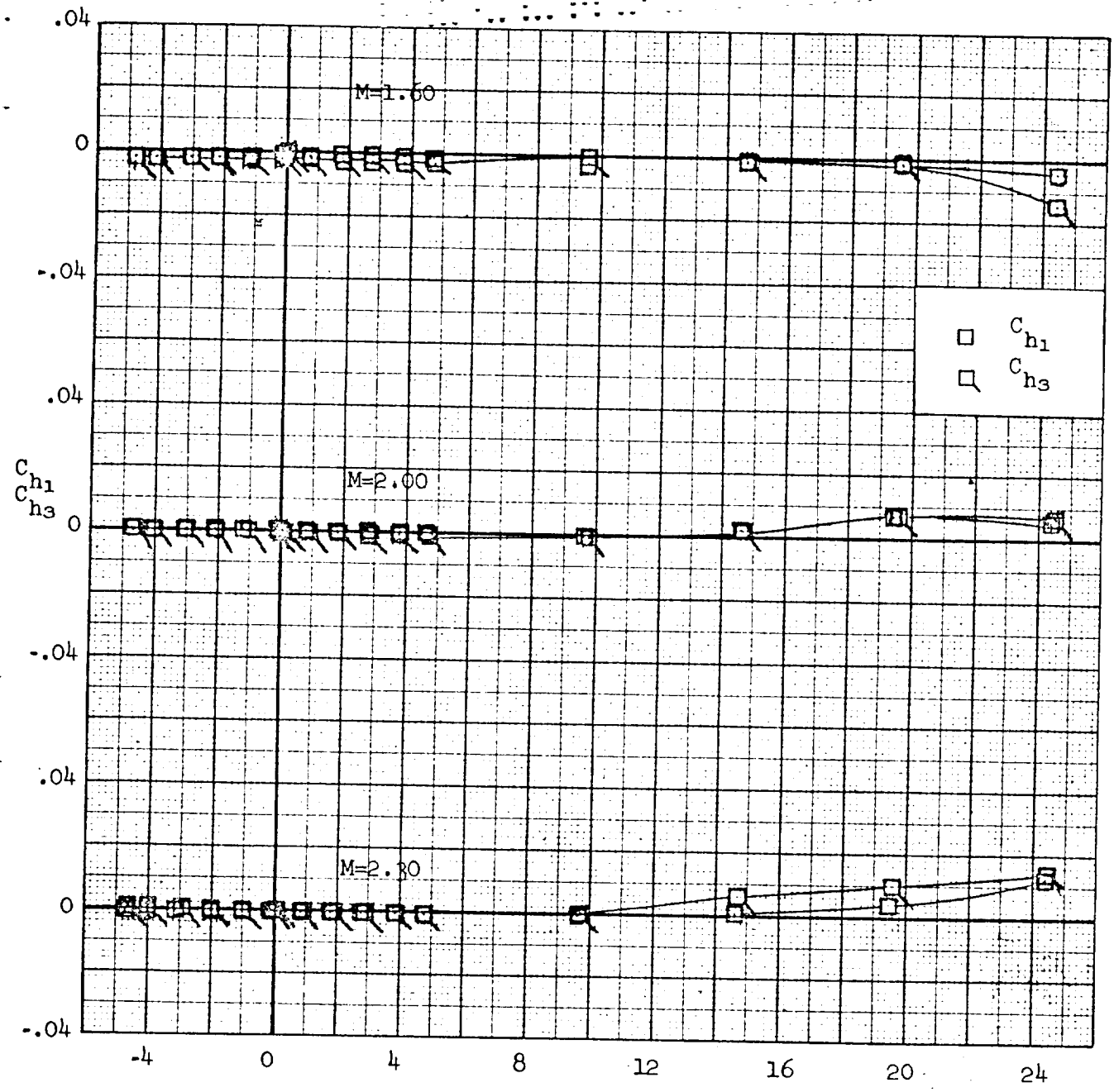

(f) Φ=22.5°

Figure 8.- Concluded.

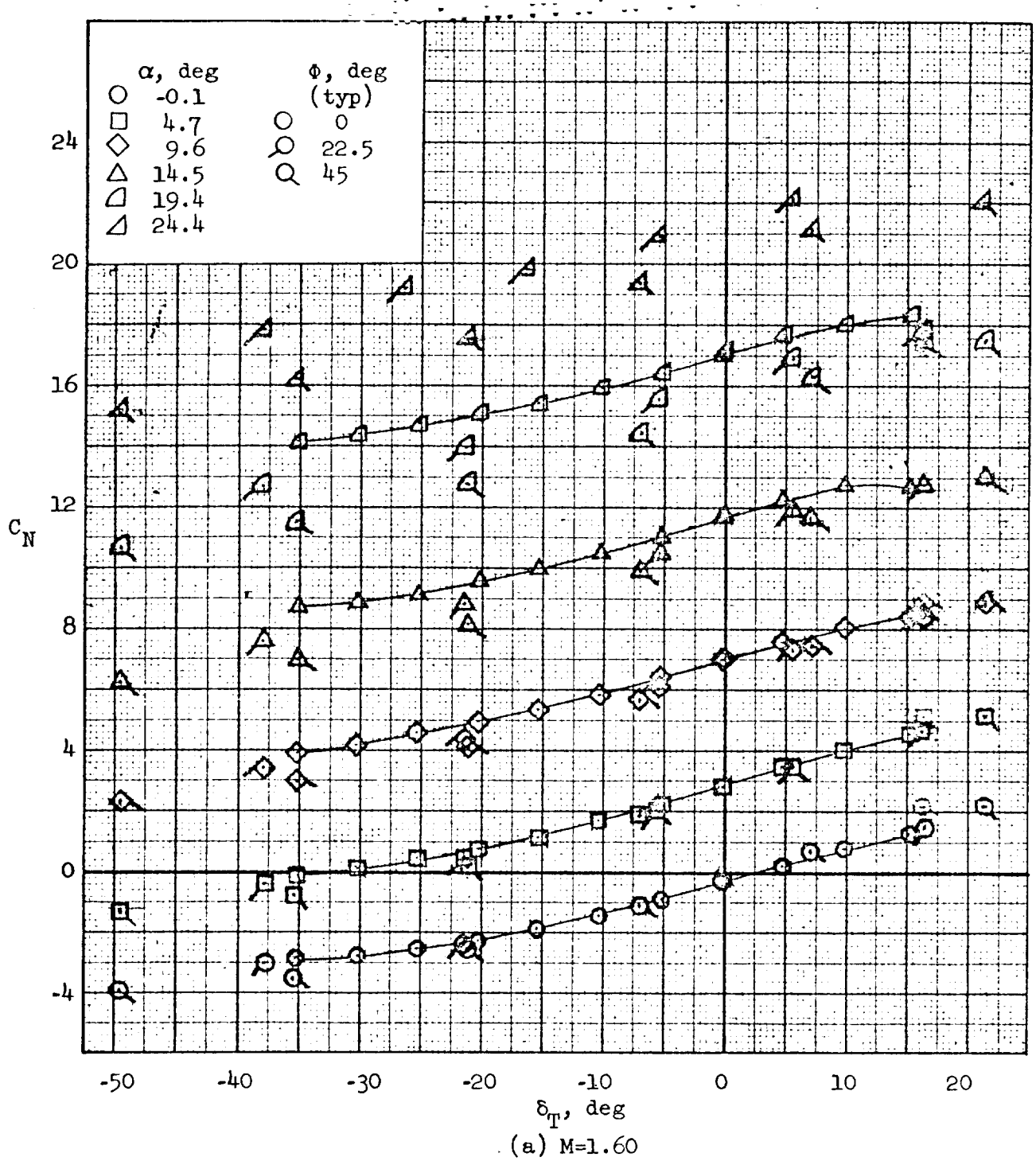

(a) M=1.60

Figure 9.- Effect of control surface deflection on normal-force coefficient for the BWE configuration.

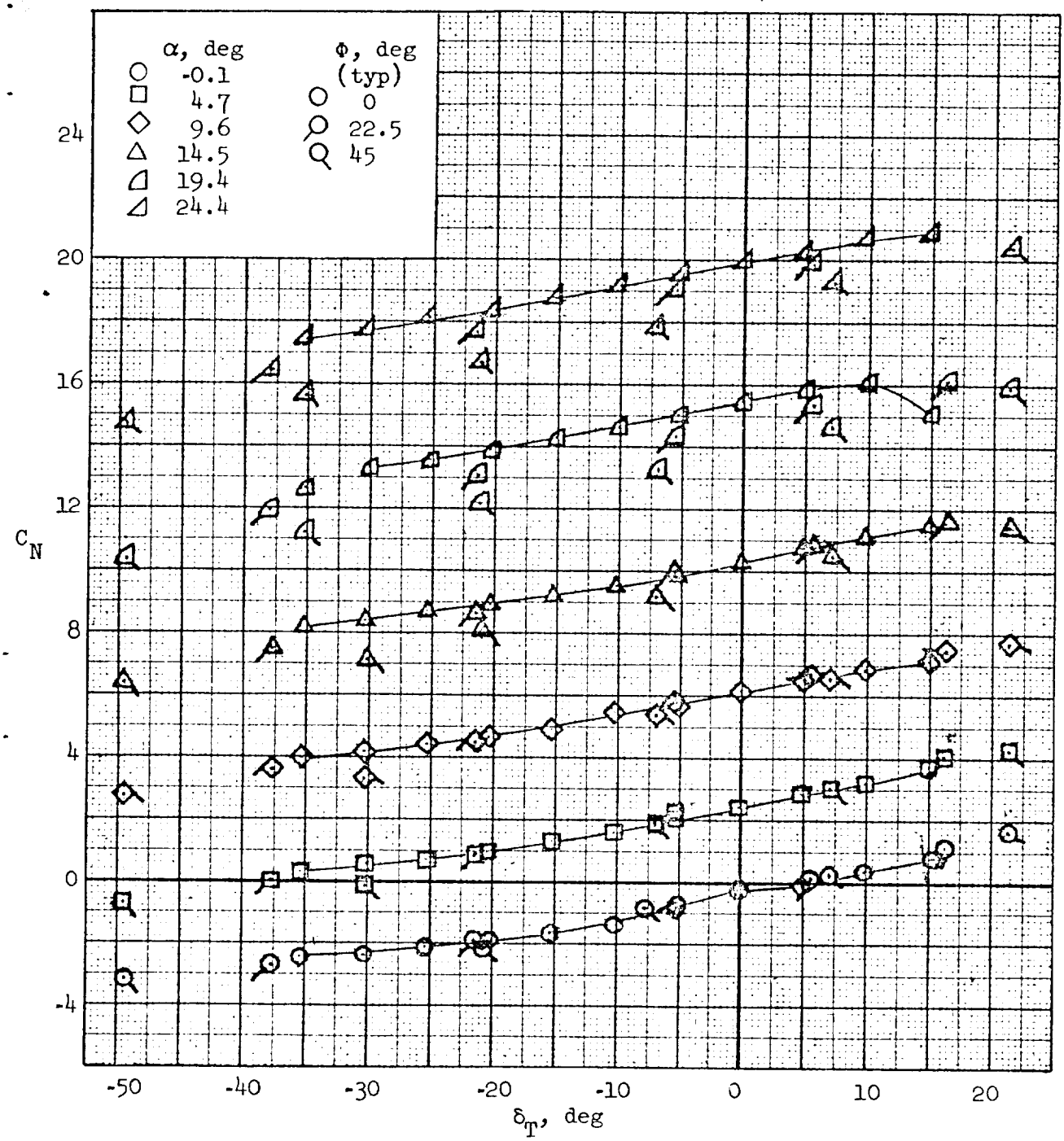

(b) M=2.00

Figure 9.- Continued.

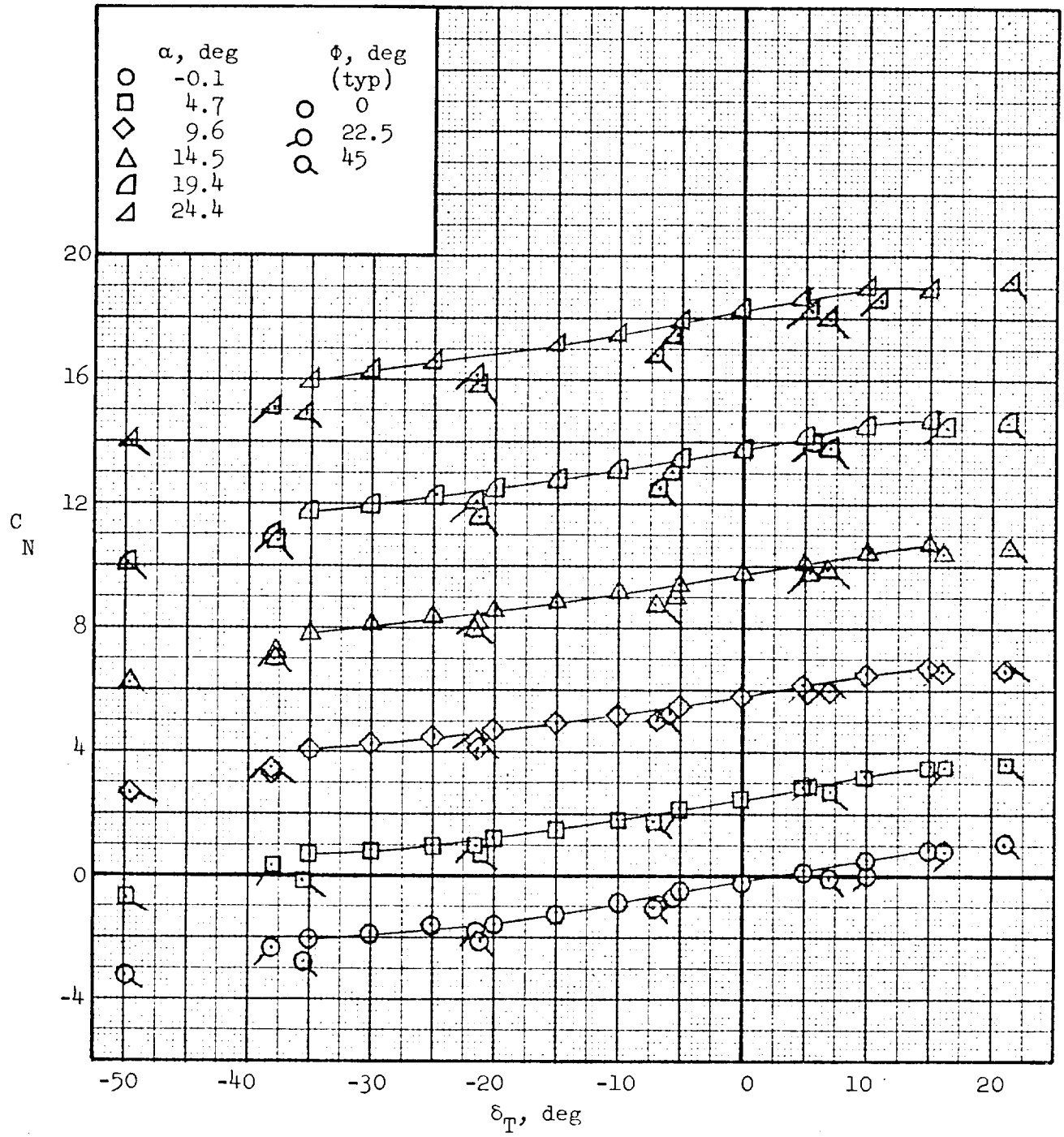

(c) M=2.30

Figure 9.- Concluded.

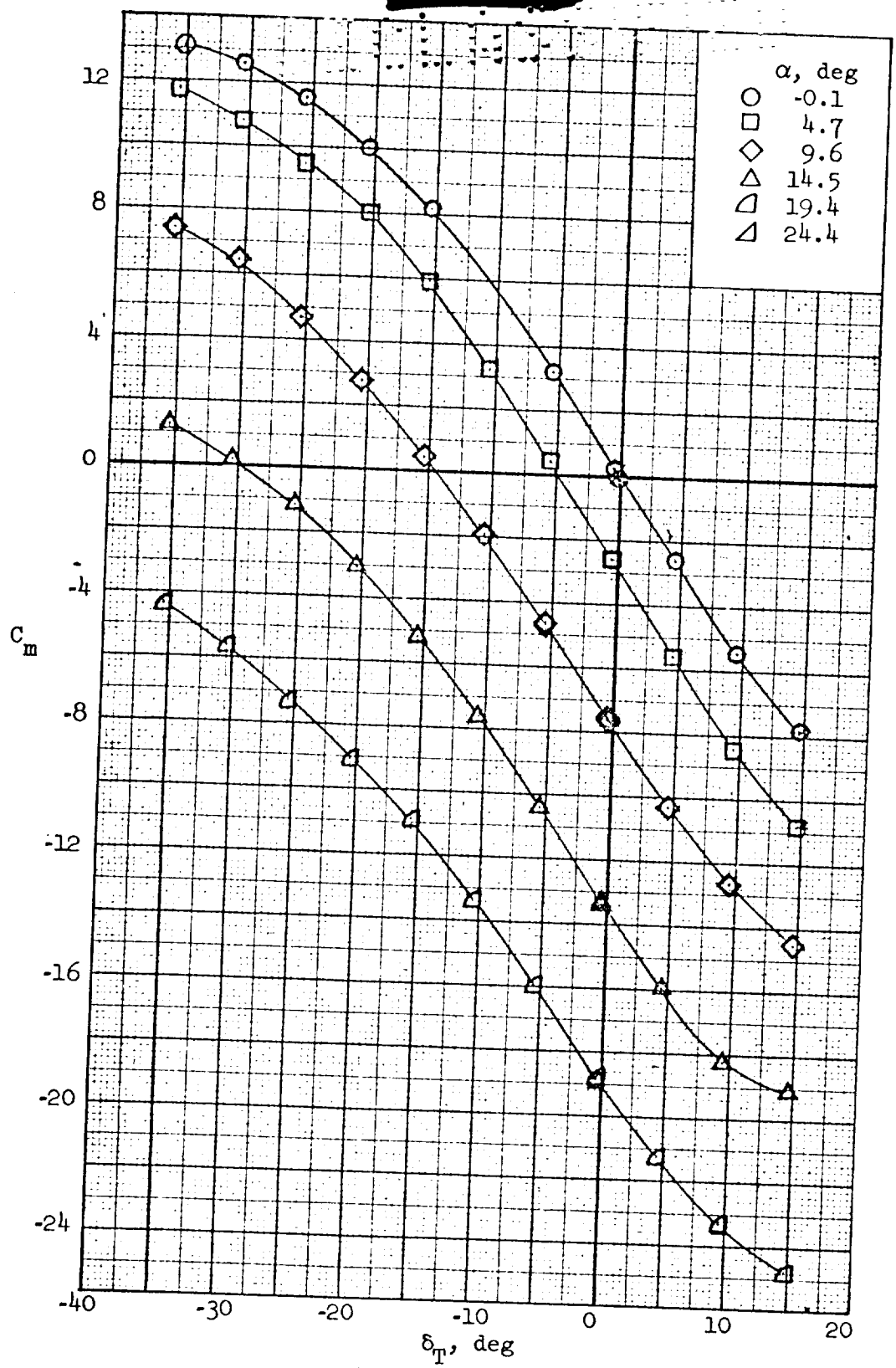

(a) M=1.60; Φ=0°

Figure 10.- Effect of control surface deflection on pitching-moment coefficient for the BWE configuration.

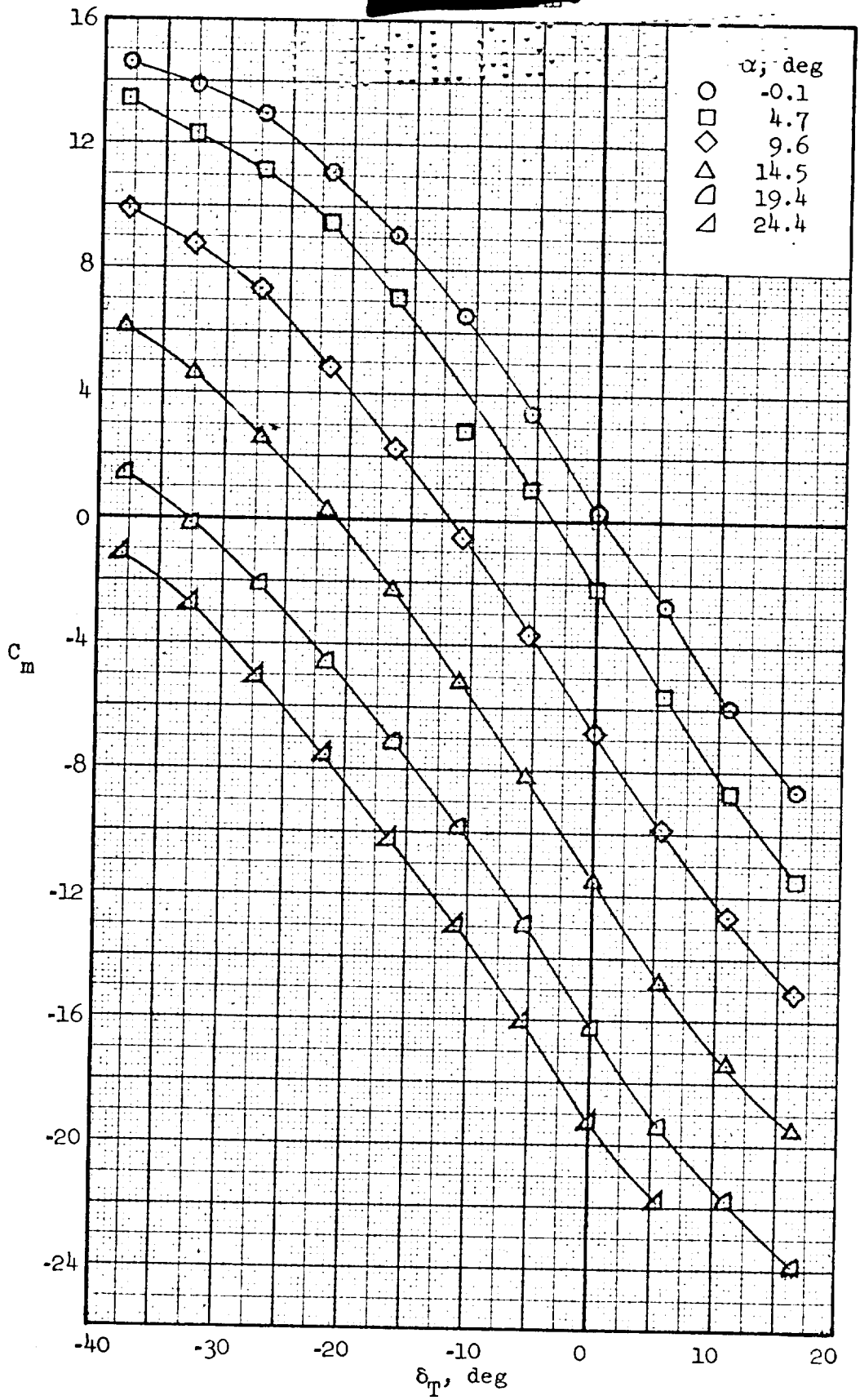

(b) M=1.60; Φ=22.5°

Figure 10.- Continued.

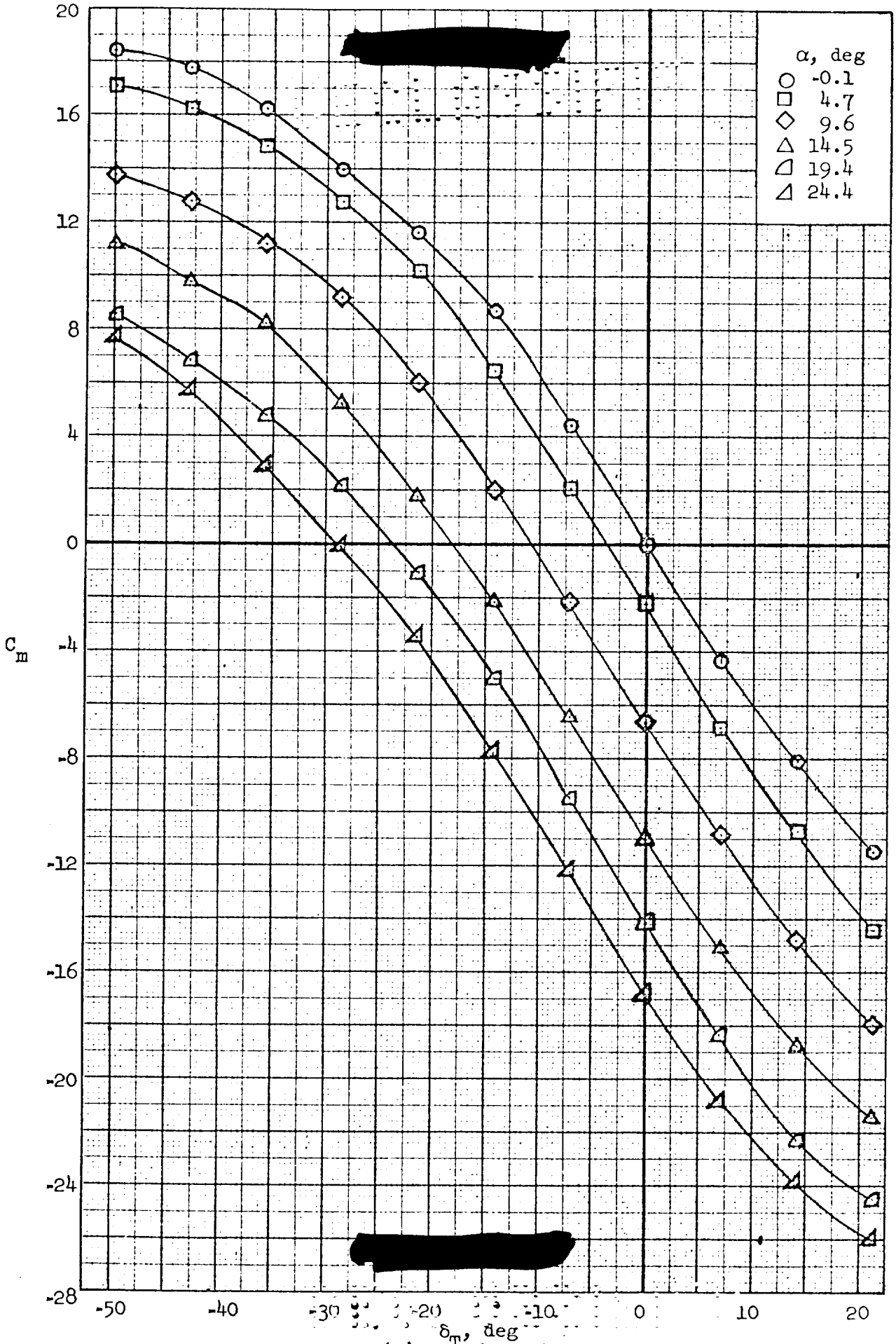

(c) M=1.60; ϕ=45°

Figure 10.- Continued.

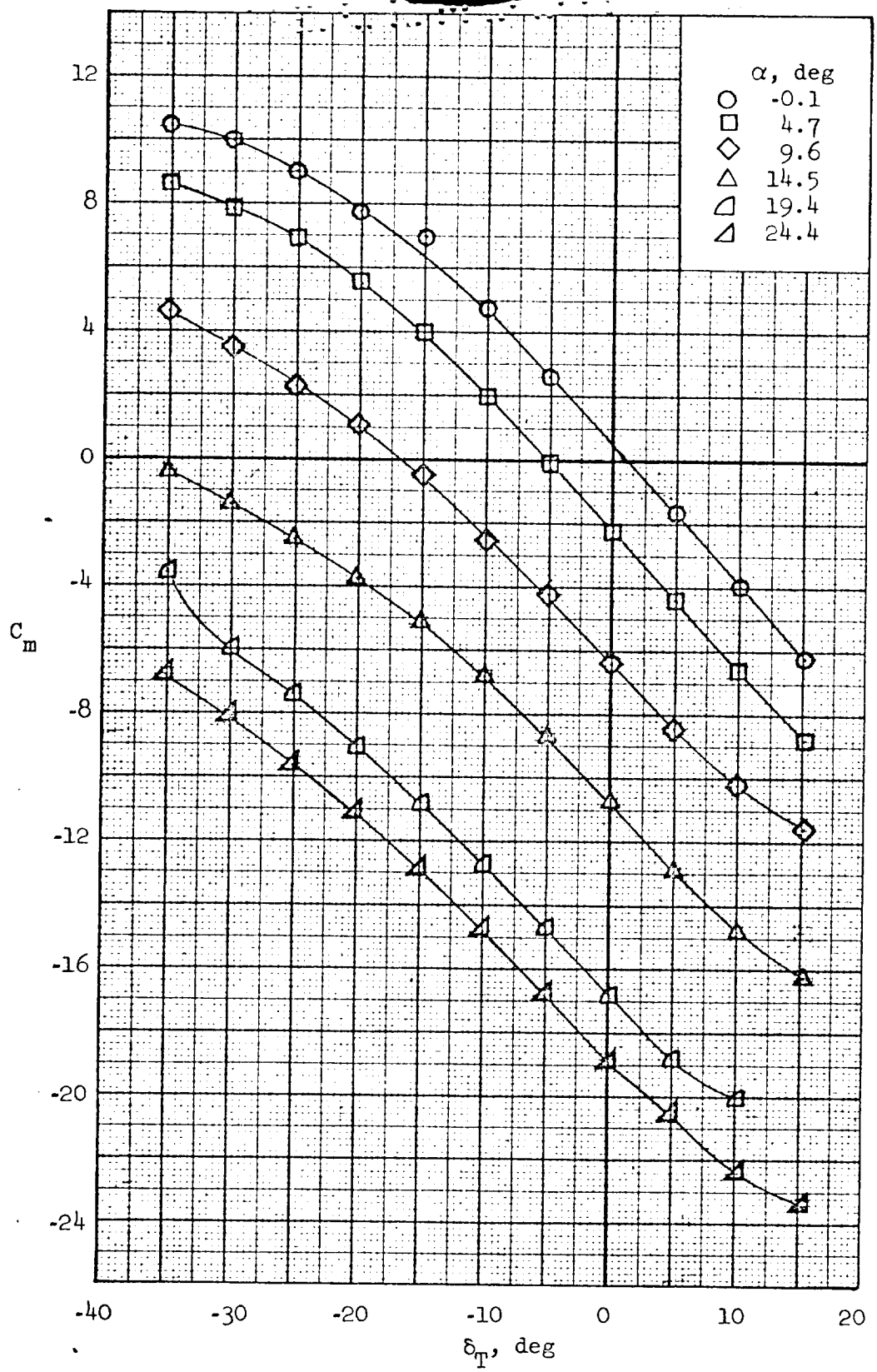

(d) M=2.00; Φ=0°

Figure 16. Continued.

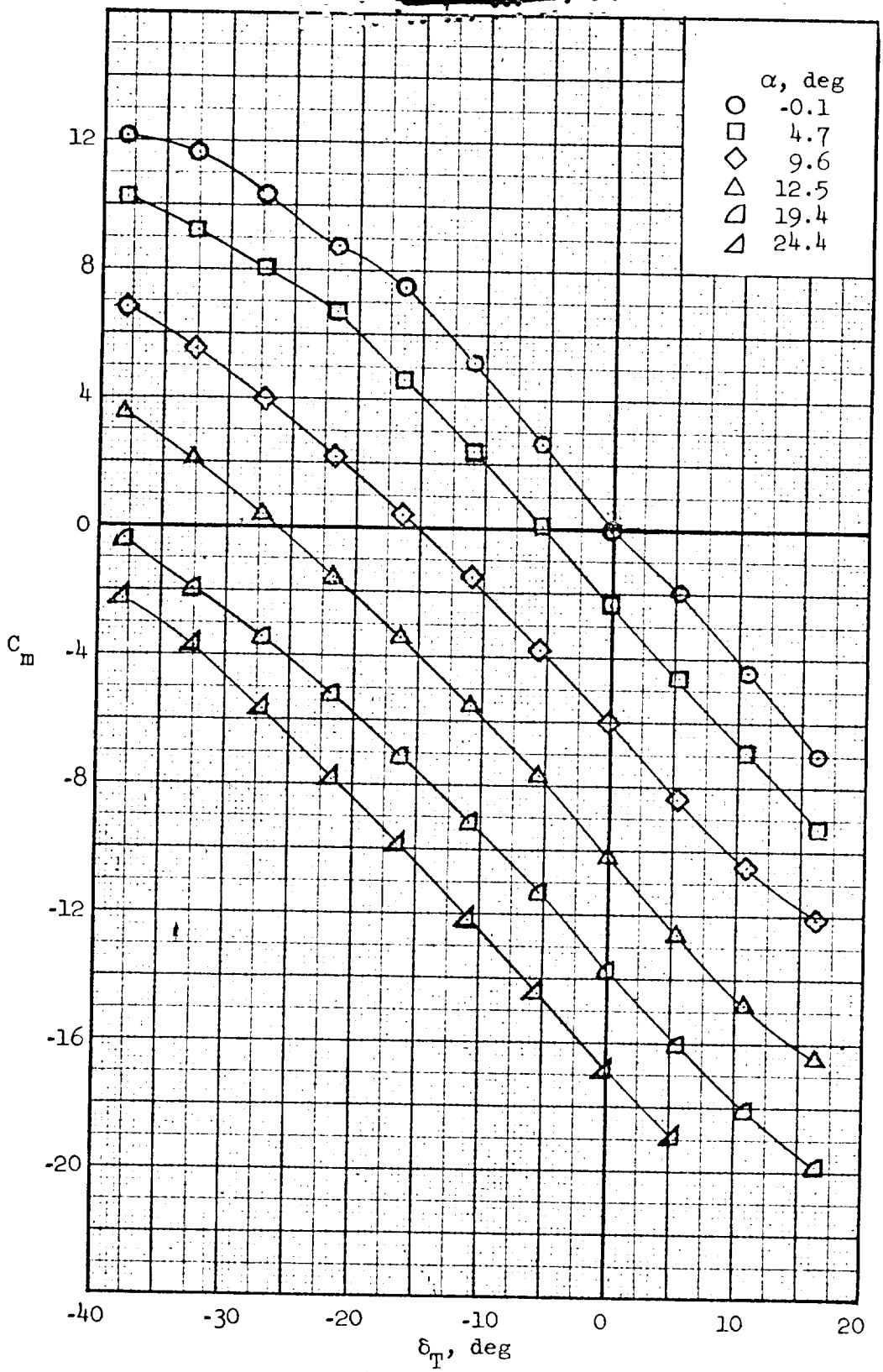

(e) M=2.00; Φ=22.5°

Figure 10.- Continued.

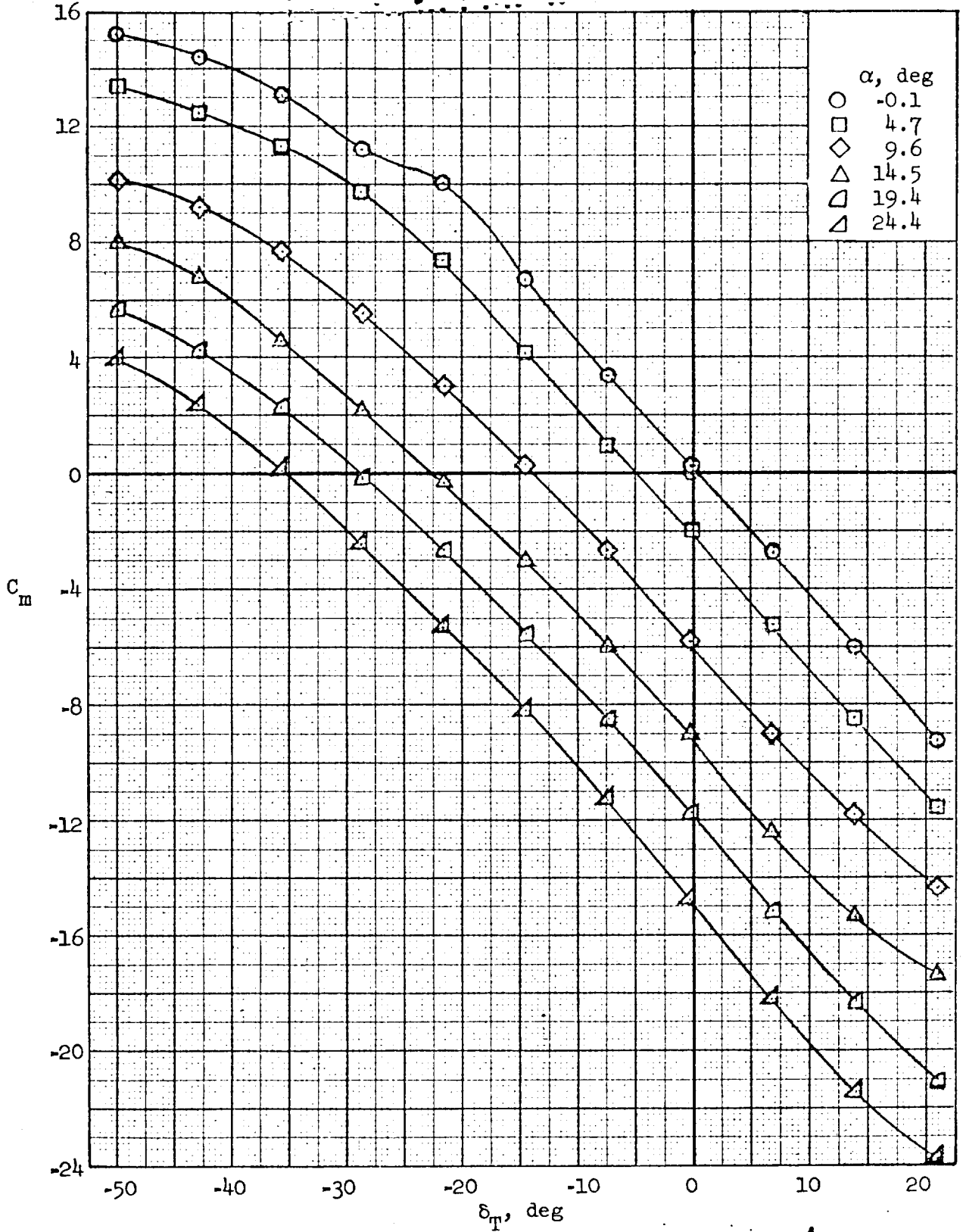

(f) M=2.00; Φ=45°

Figure 10.- Continued.

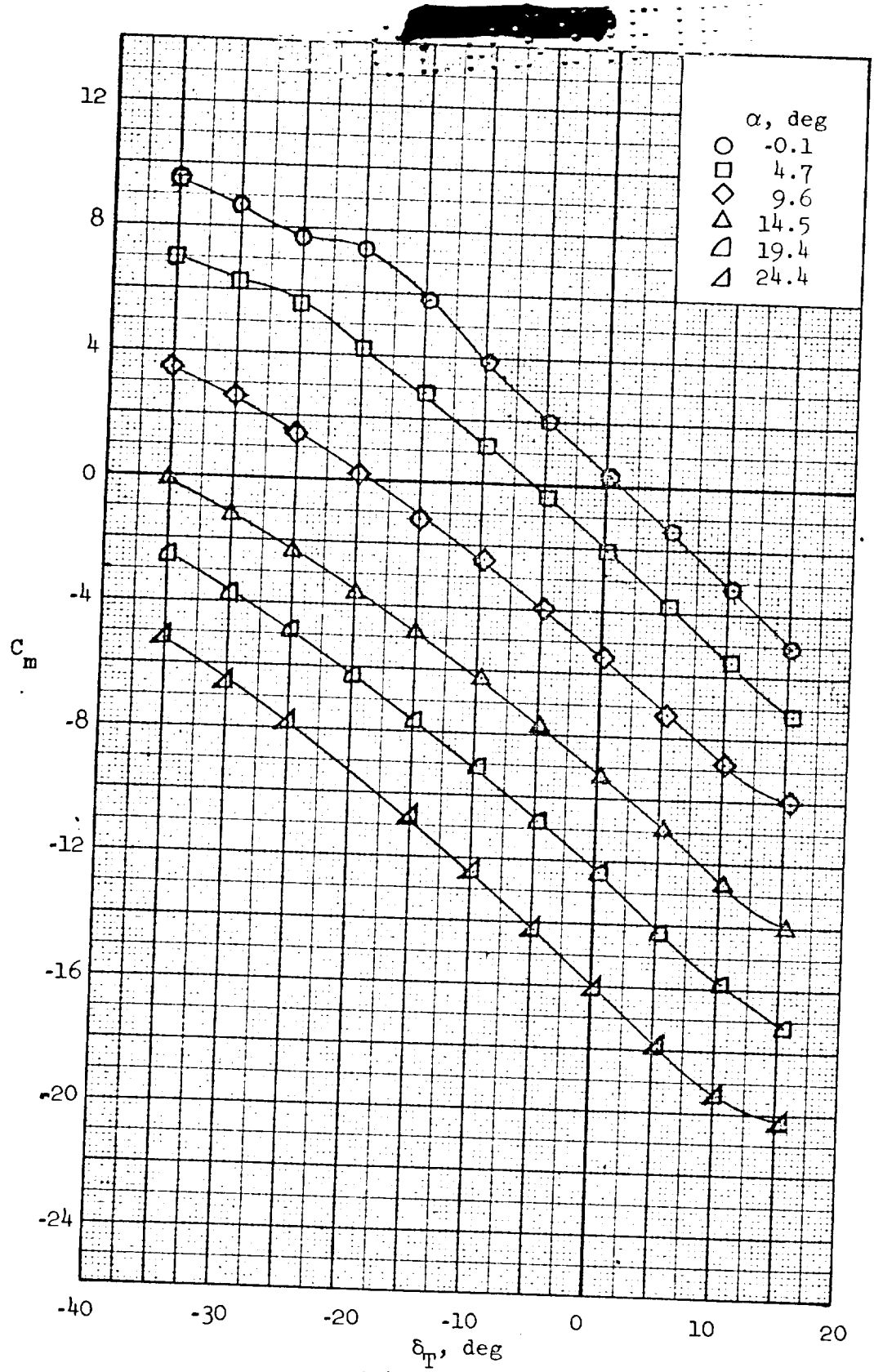

(g) M=2.30; Φ=0°

Figure 10.- Continued.

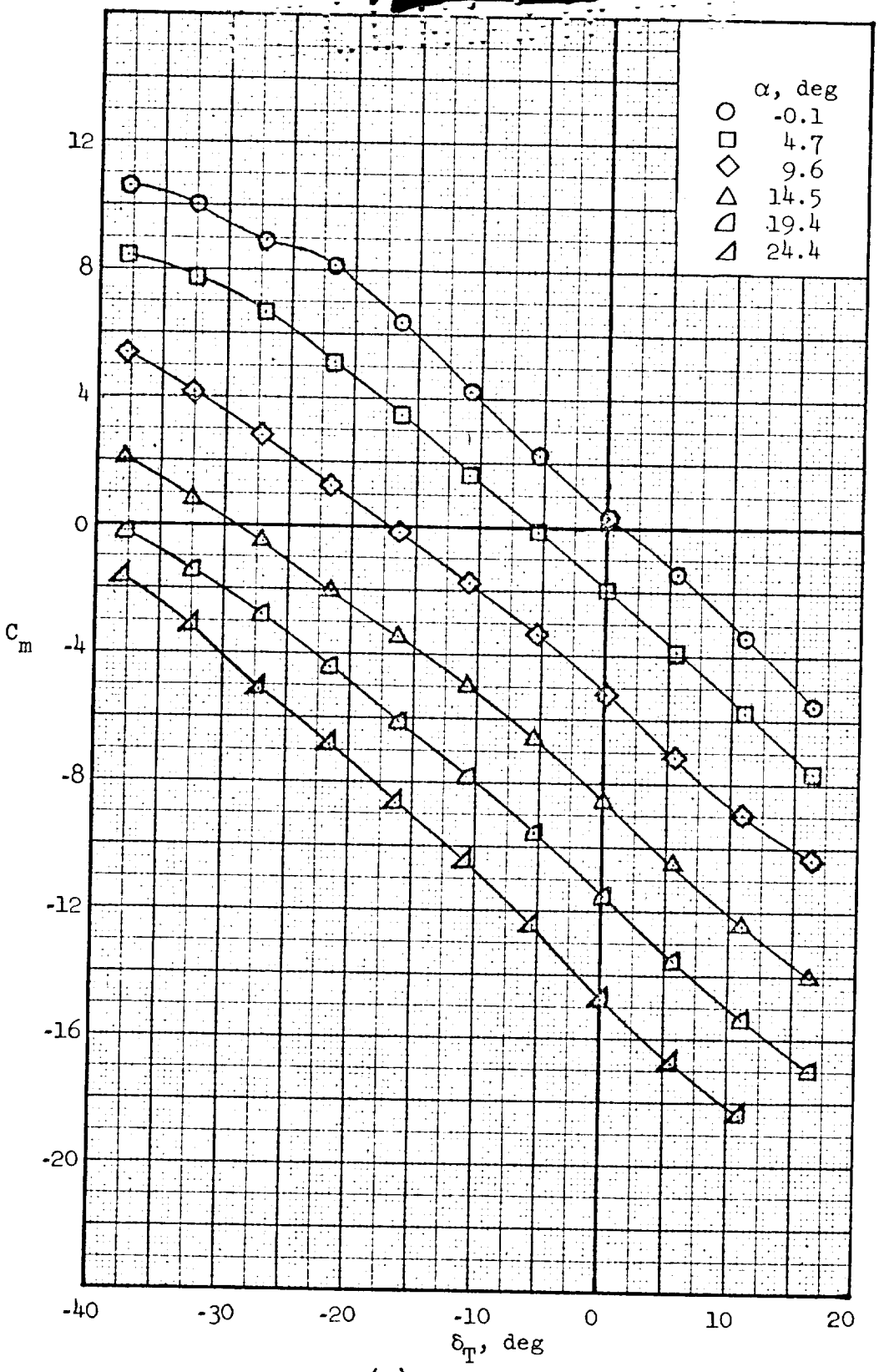

(h) M=2.30; Φ=22.5°

Figure 10. - Continued.

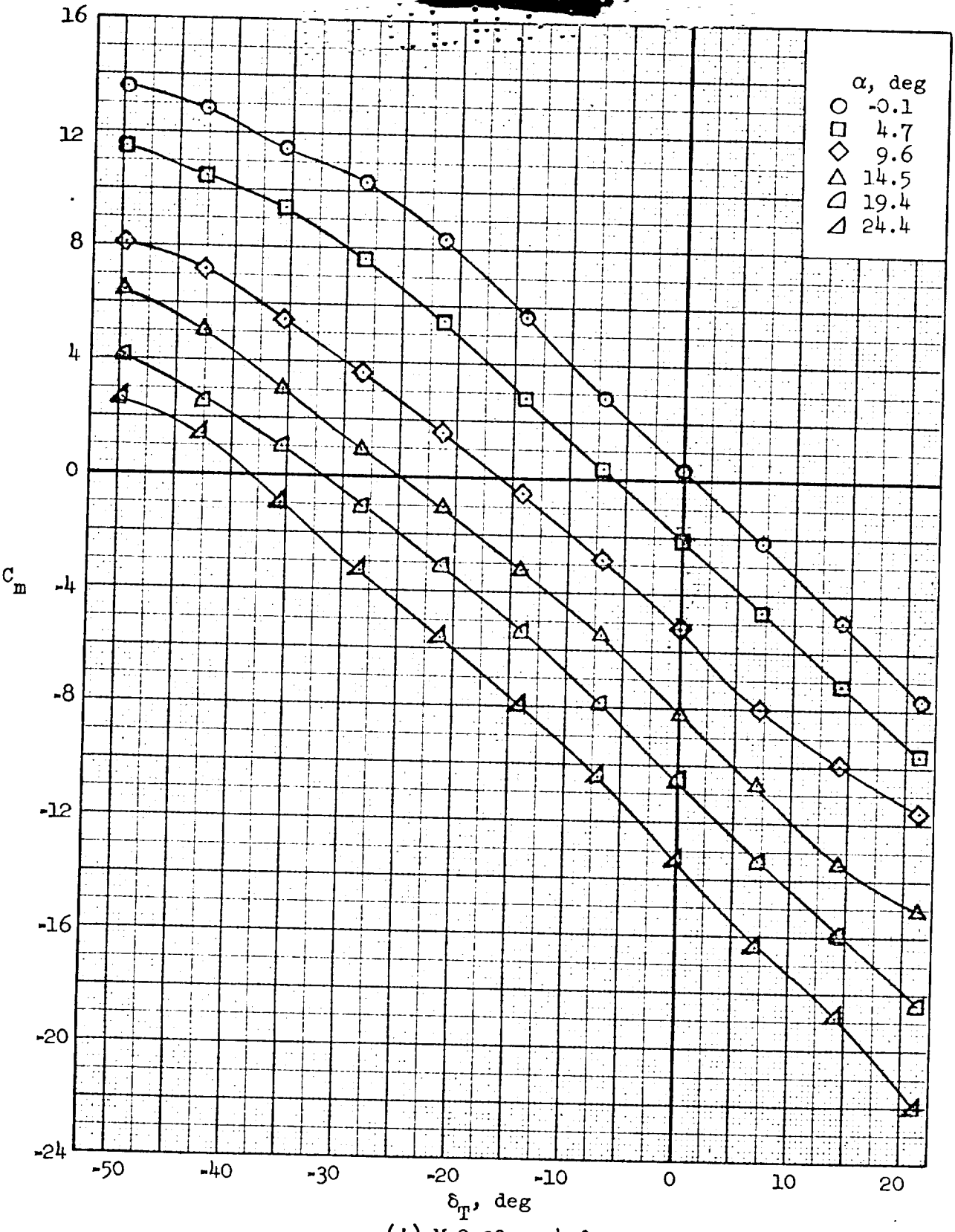

(i) M=2.30; Φ=45°

Figure 10.- Concluded.

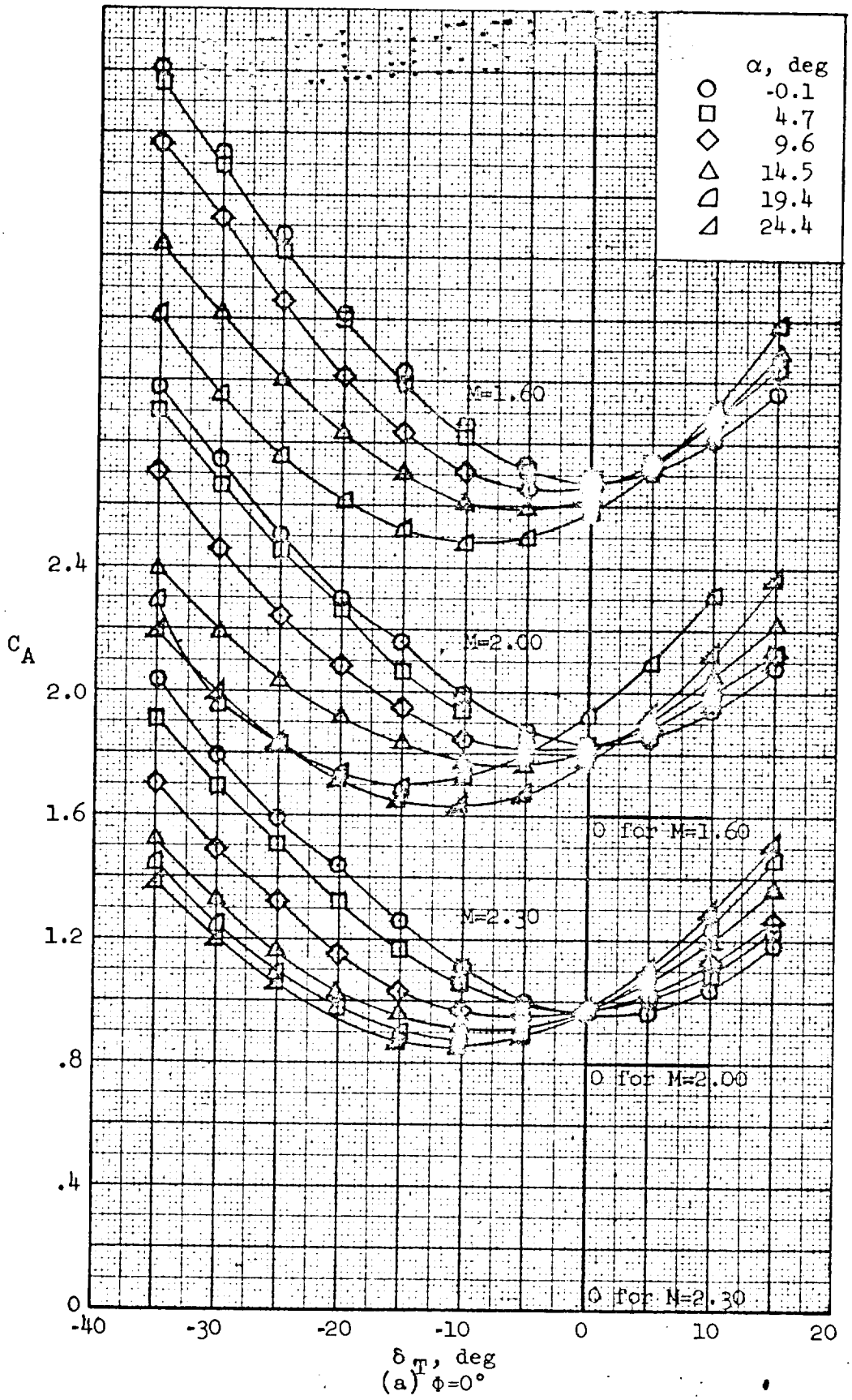

Figure 11.- Effect of control surface deflection on axial-force coefficient for the BWE configuration.

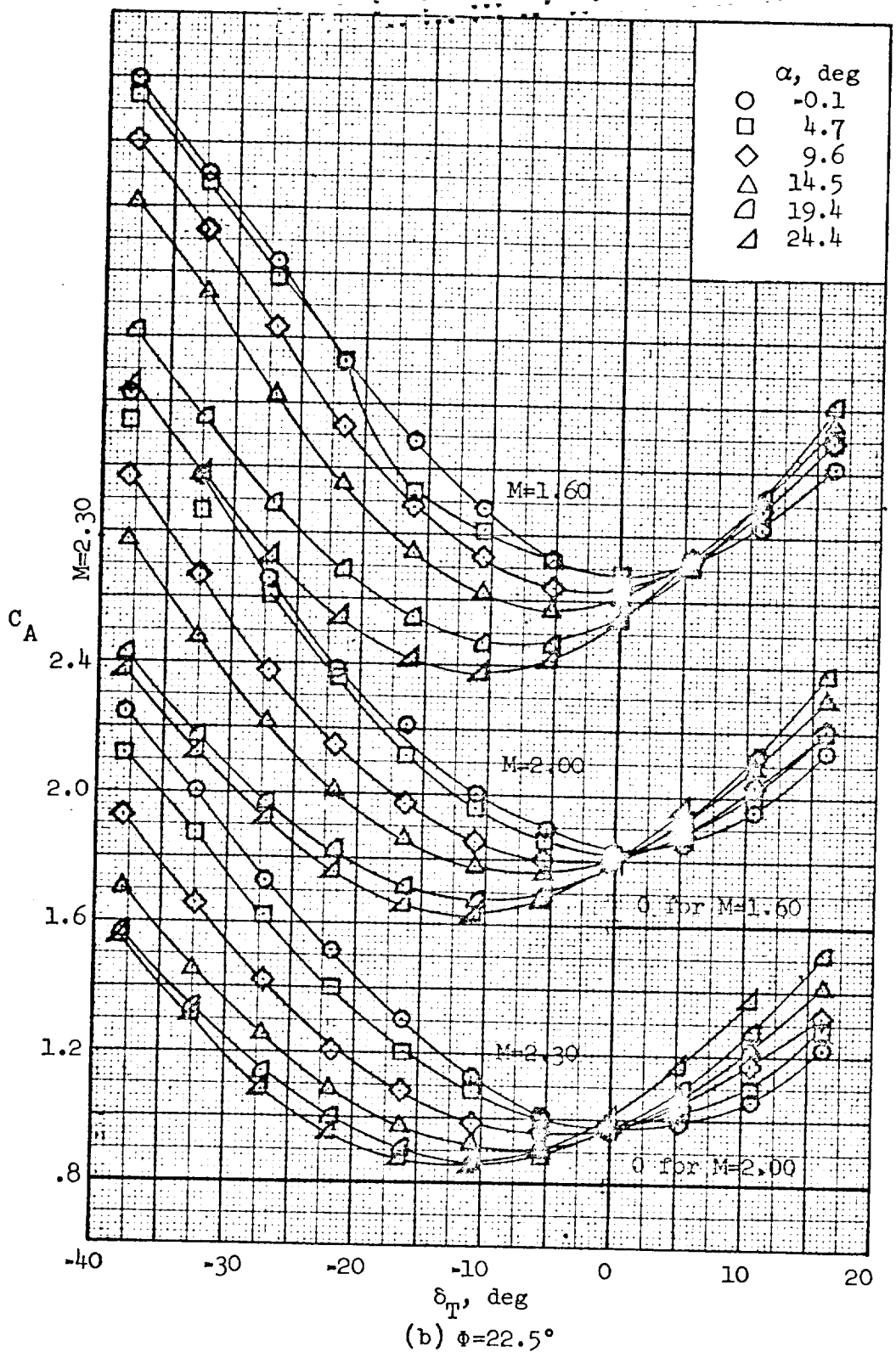

(b) Φ=22.5°

Figure 11.- Continued.

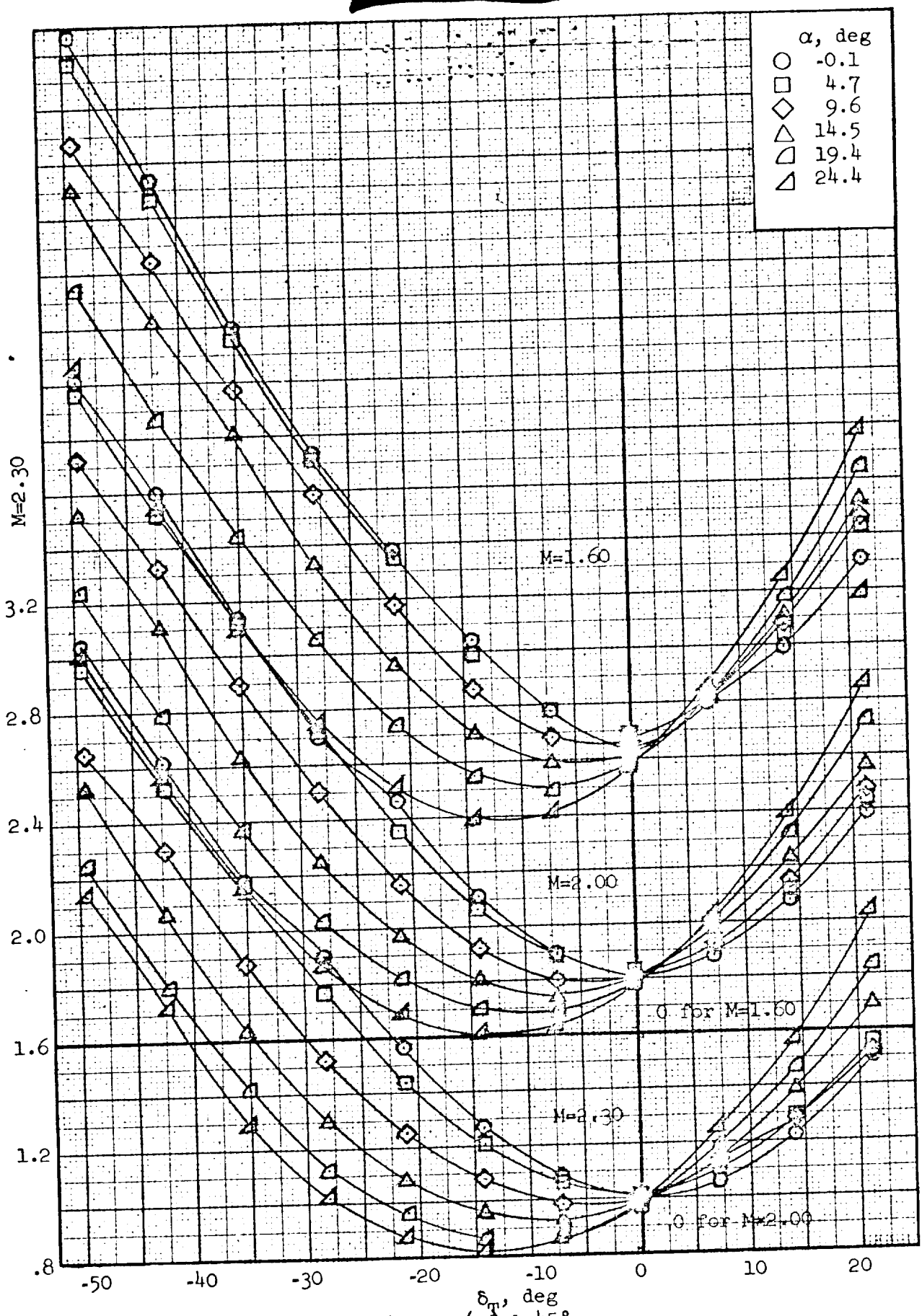

(c) ϕ=45°

Figure 11. Concluded

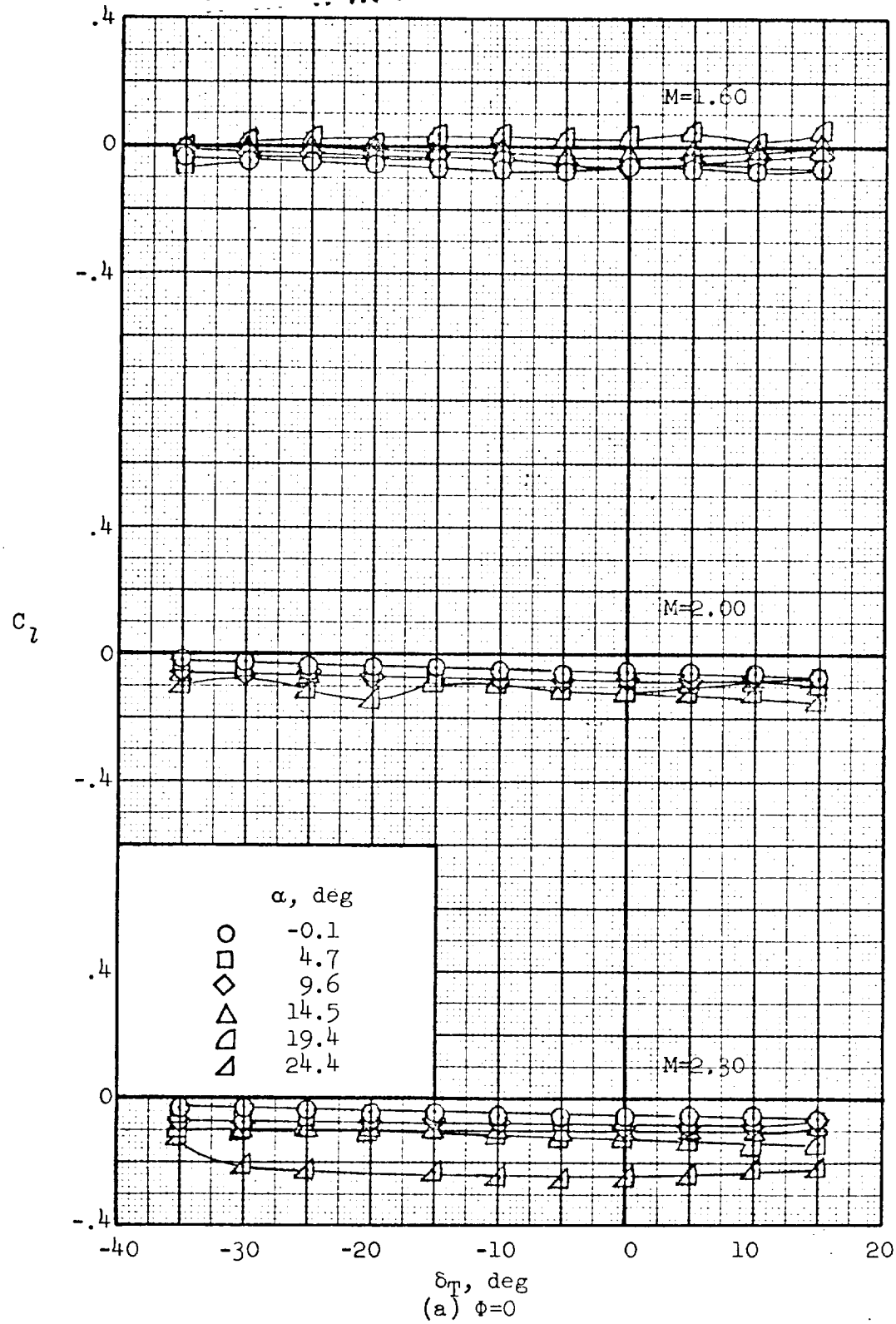

(a) Φ=0

Figure 12.- Effect of control surface deflection on rolling-moment coefficient for the BWE configuration.

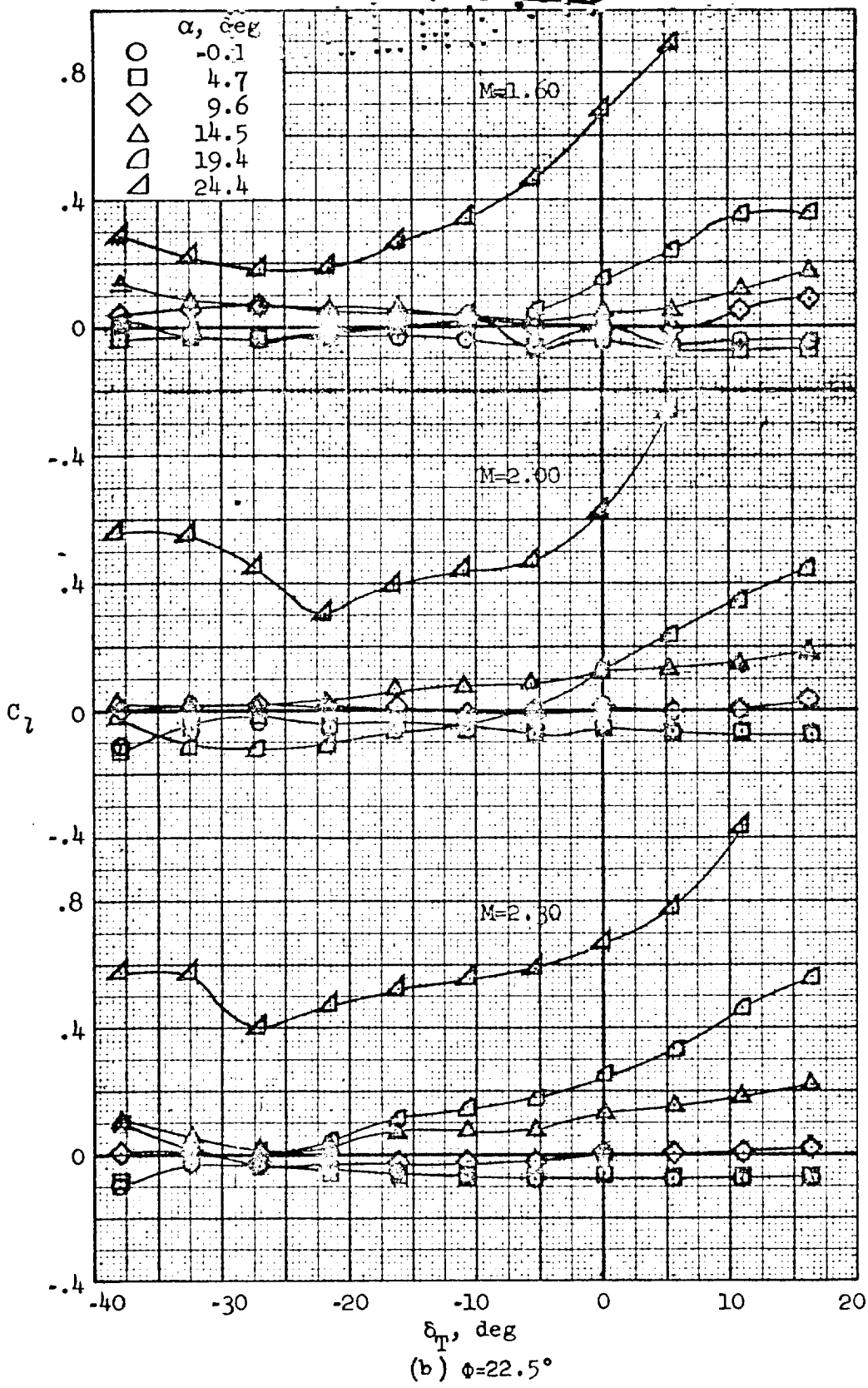

(b) Φ=22.5°

Figure 12.- Concluded.

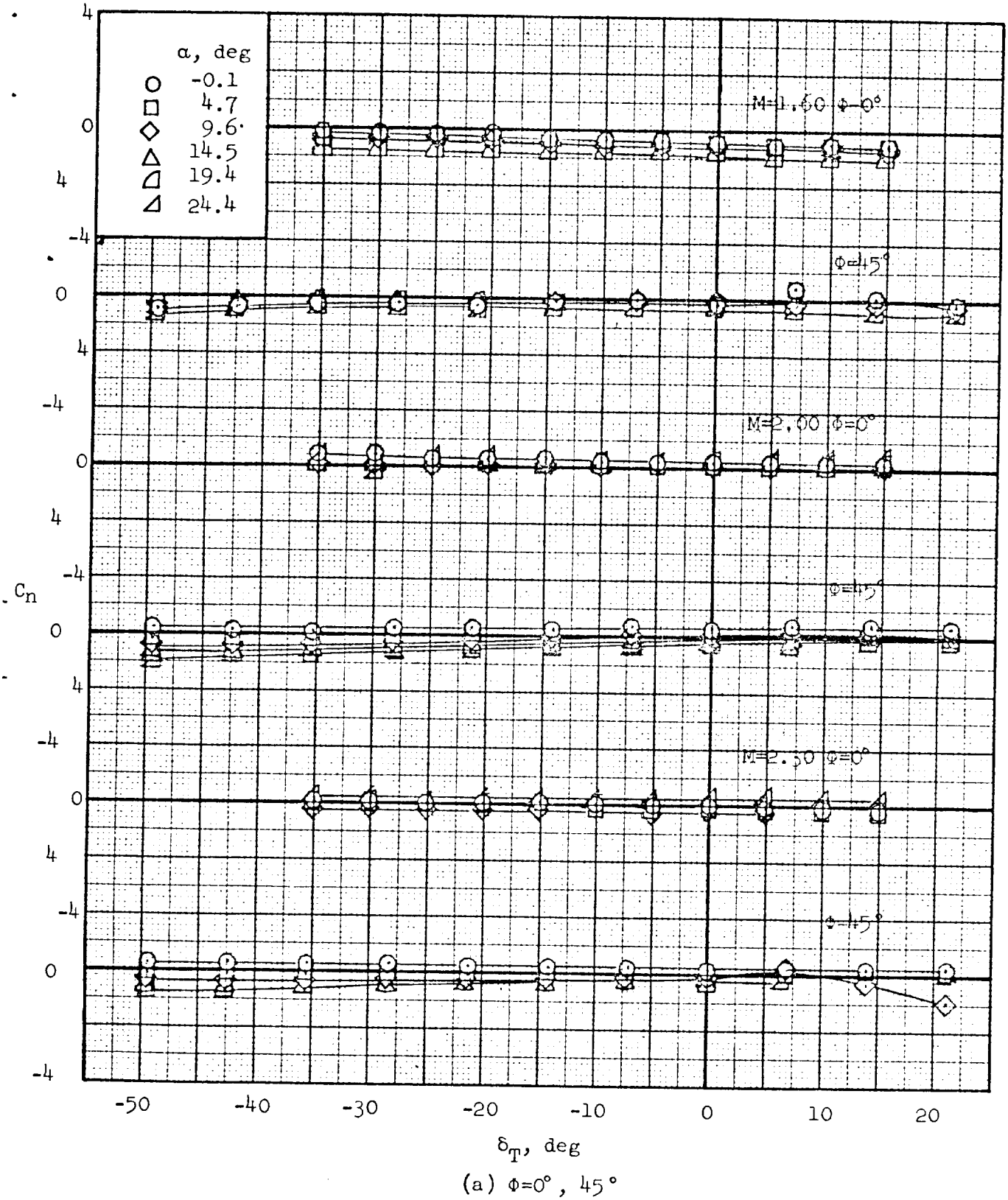

(a) Φ=0°, 45°

Figure 13.- Effect of control surface deflection on yawing-moment coefficient for the BWB configuration.

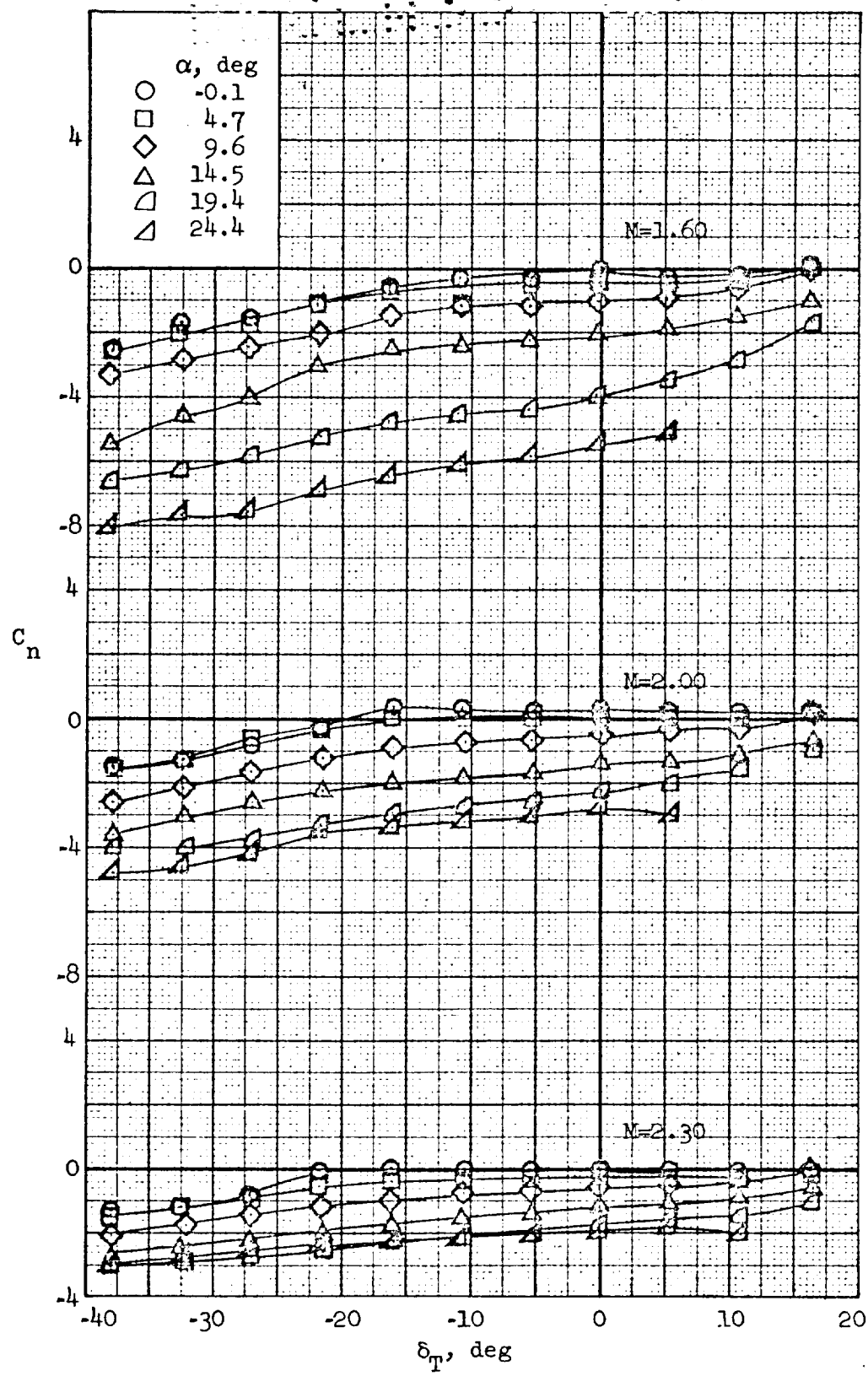

(b) Φ=22.5°

Figure 13.- Concluded.

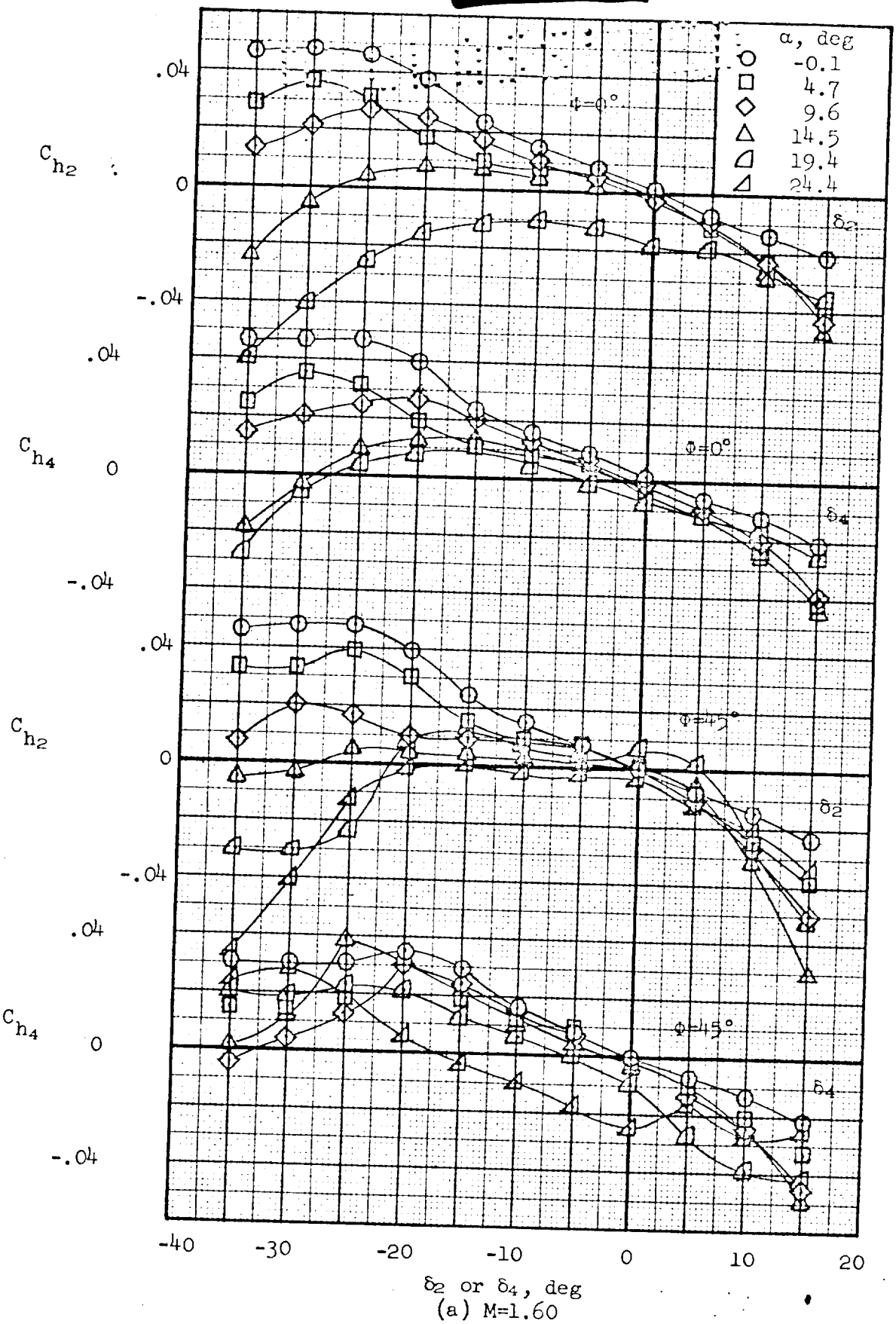

(a) M=1.60

Figure 14.- Hinge moment characteristics at Φ=0° and 45° for the [redacted] configuration.

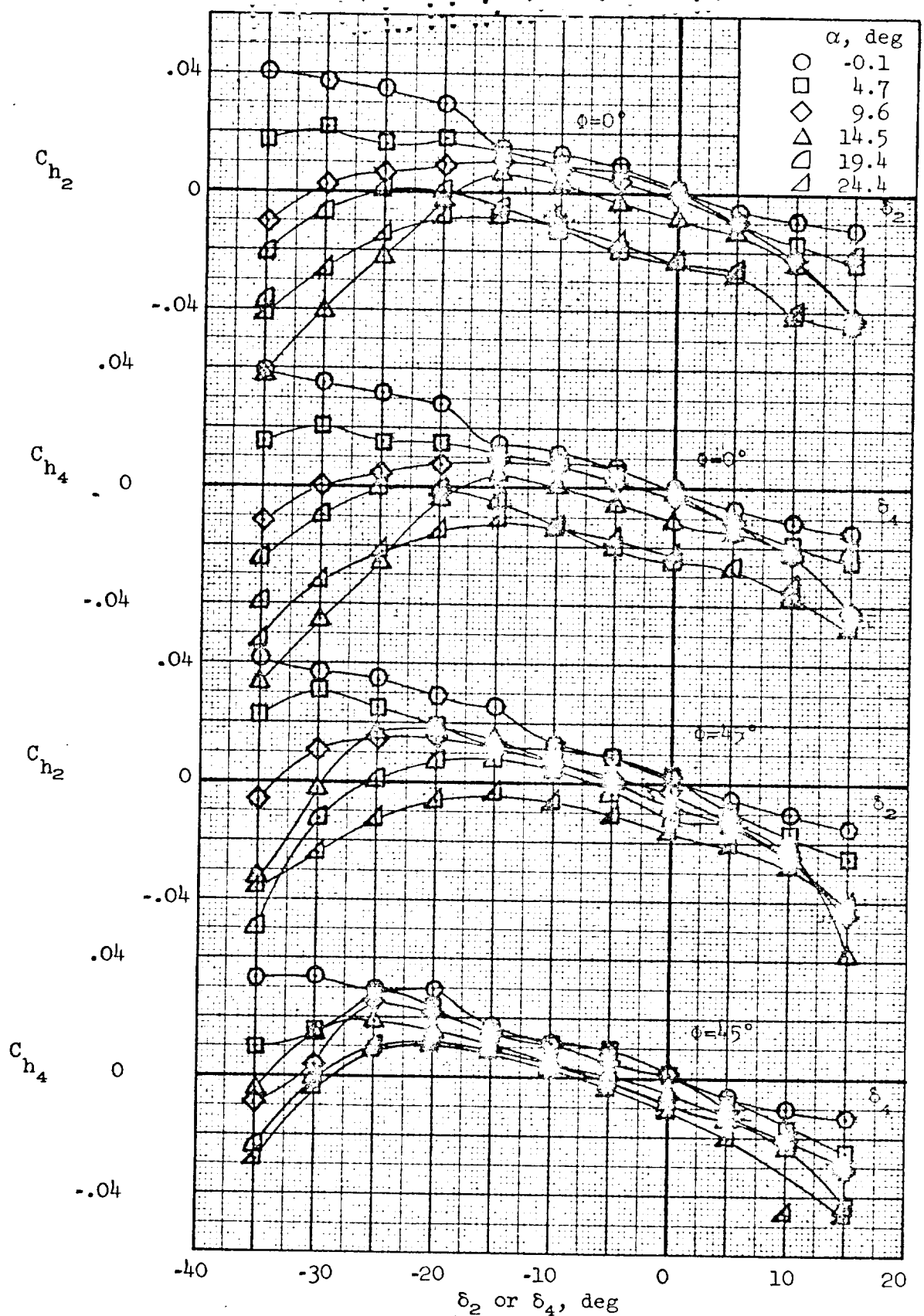

(b) M=2.00

Figure 14. Continued.

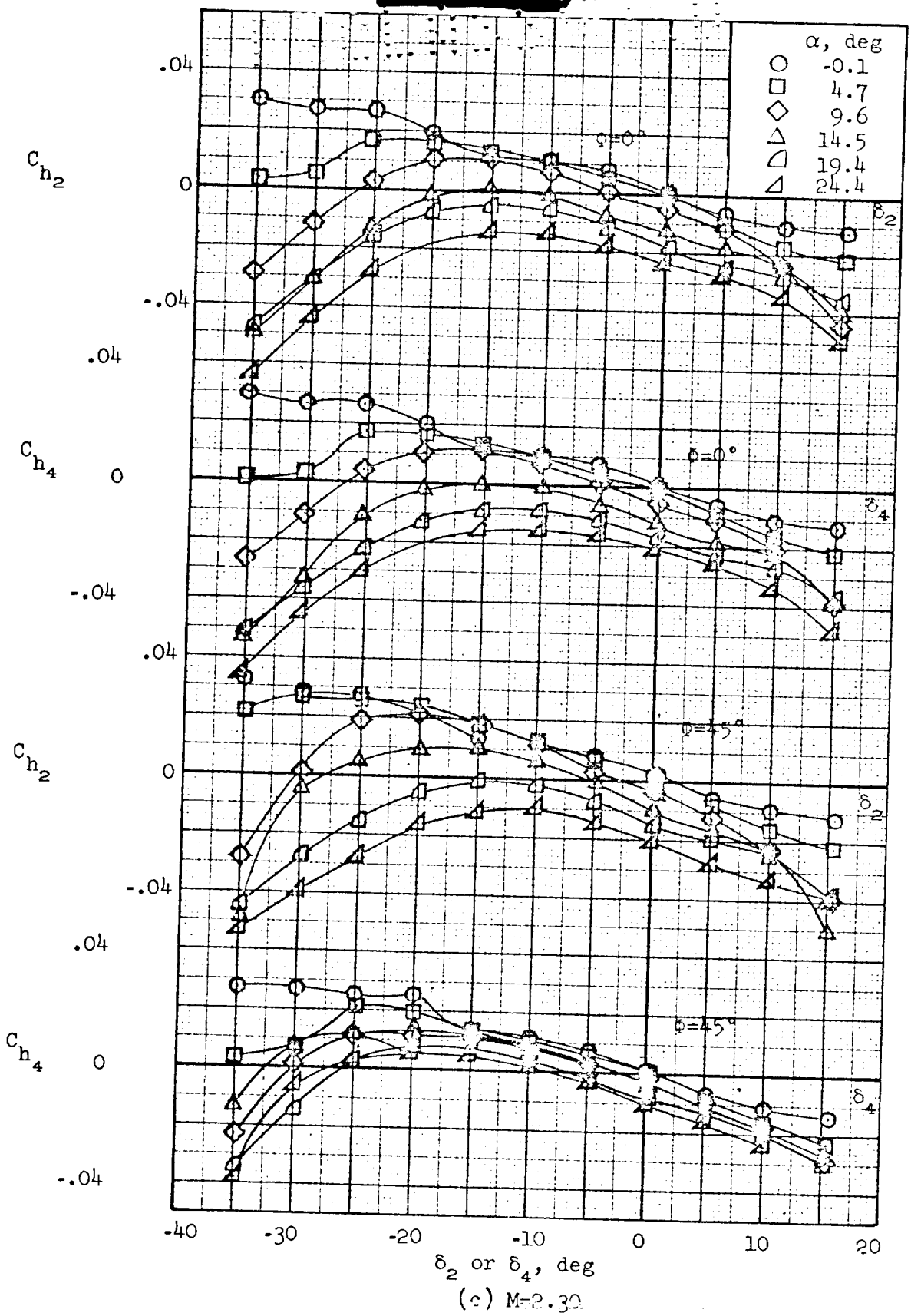

(c) M=2.30

Figure 14. Concluded.

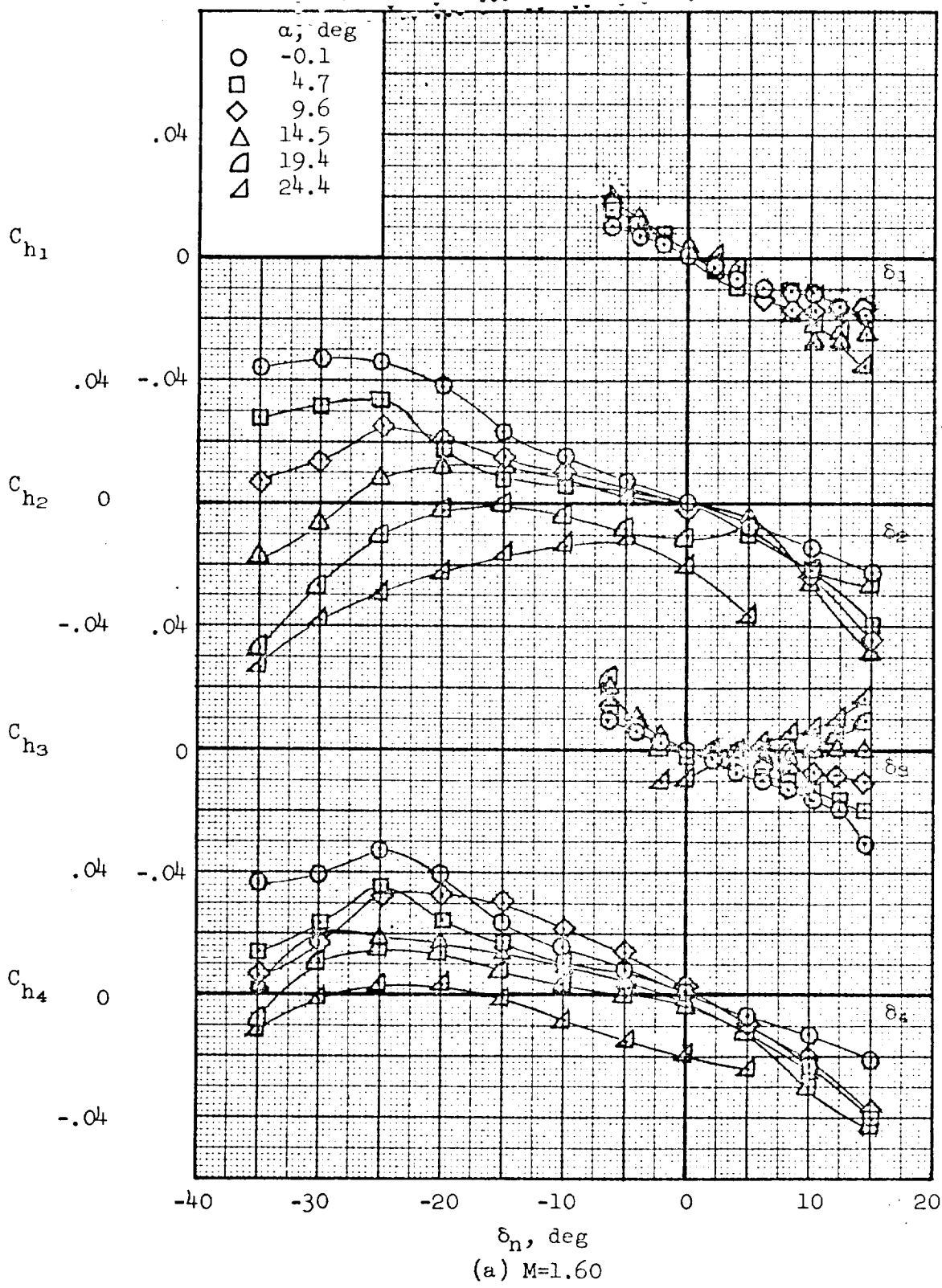

(a) M=1.60

Figure 15.- Hinge moment characteristics at Φ=22.5° for the BWE configuration.

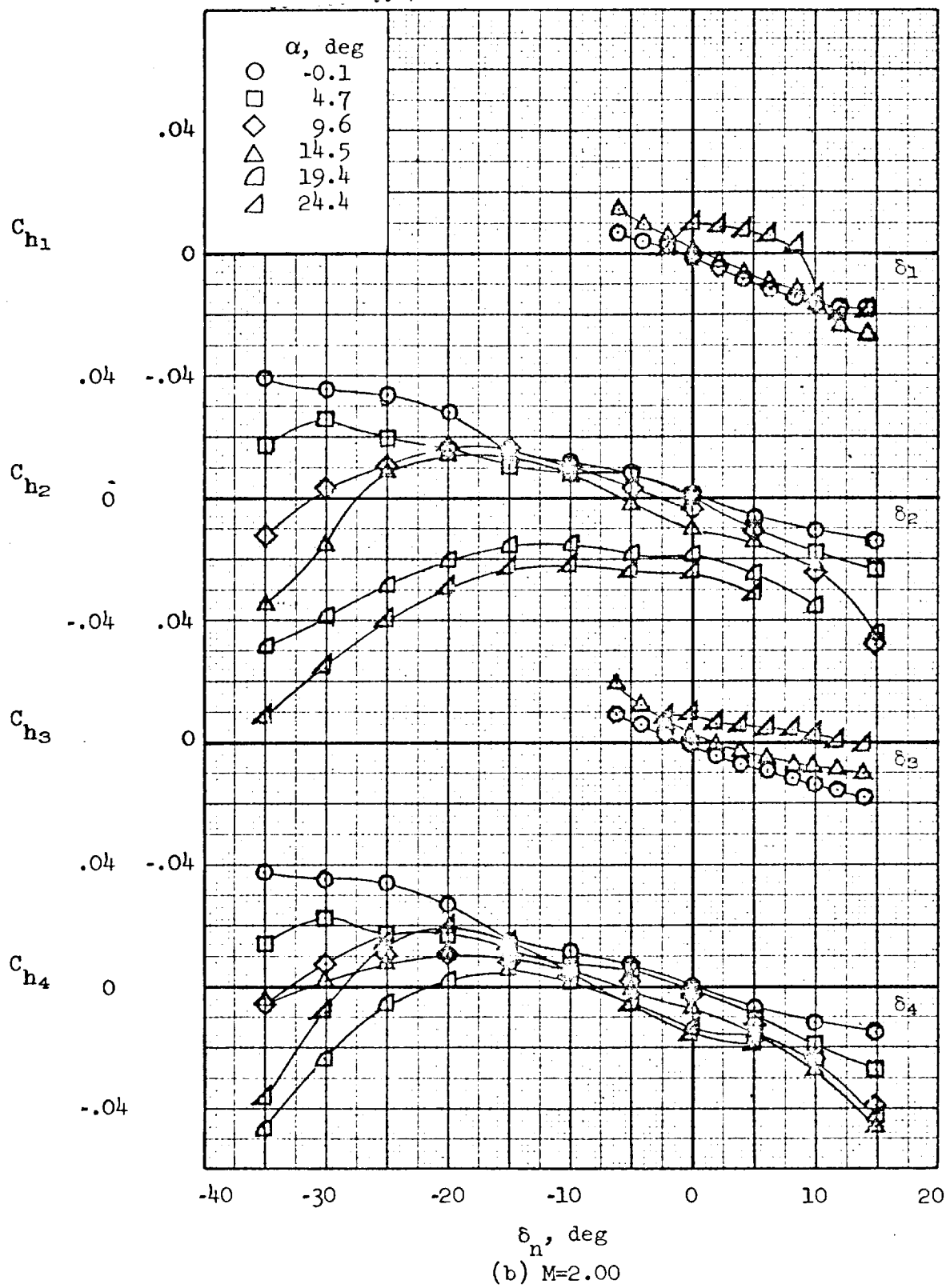

(b) M=2.00

Figure 15.- Continued.

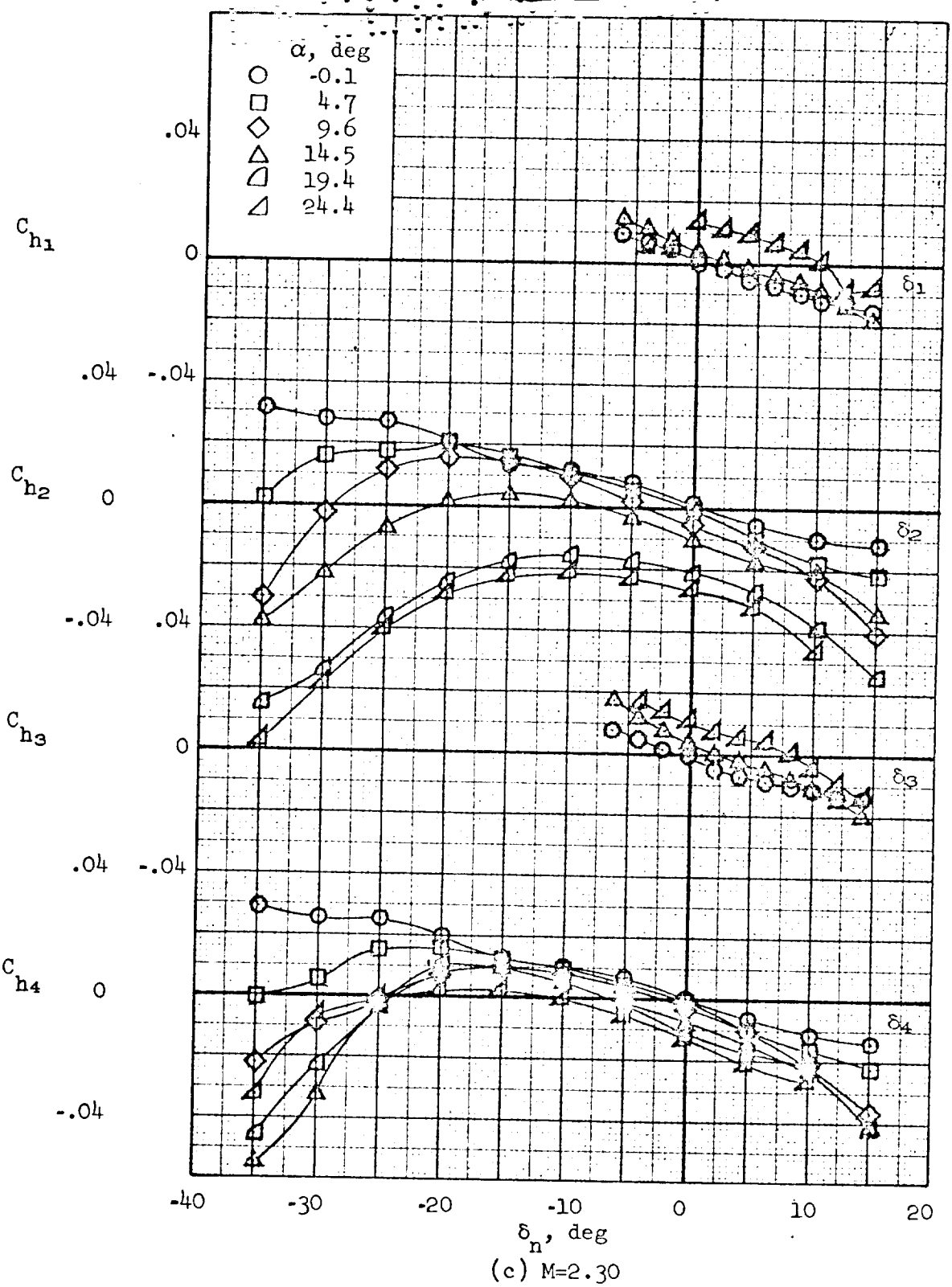

(c) M=2.30

Figure 15.- Concluded.

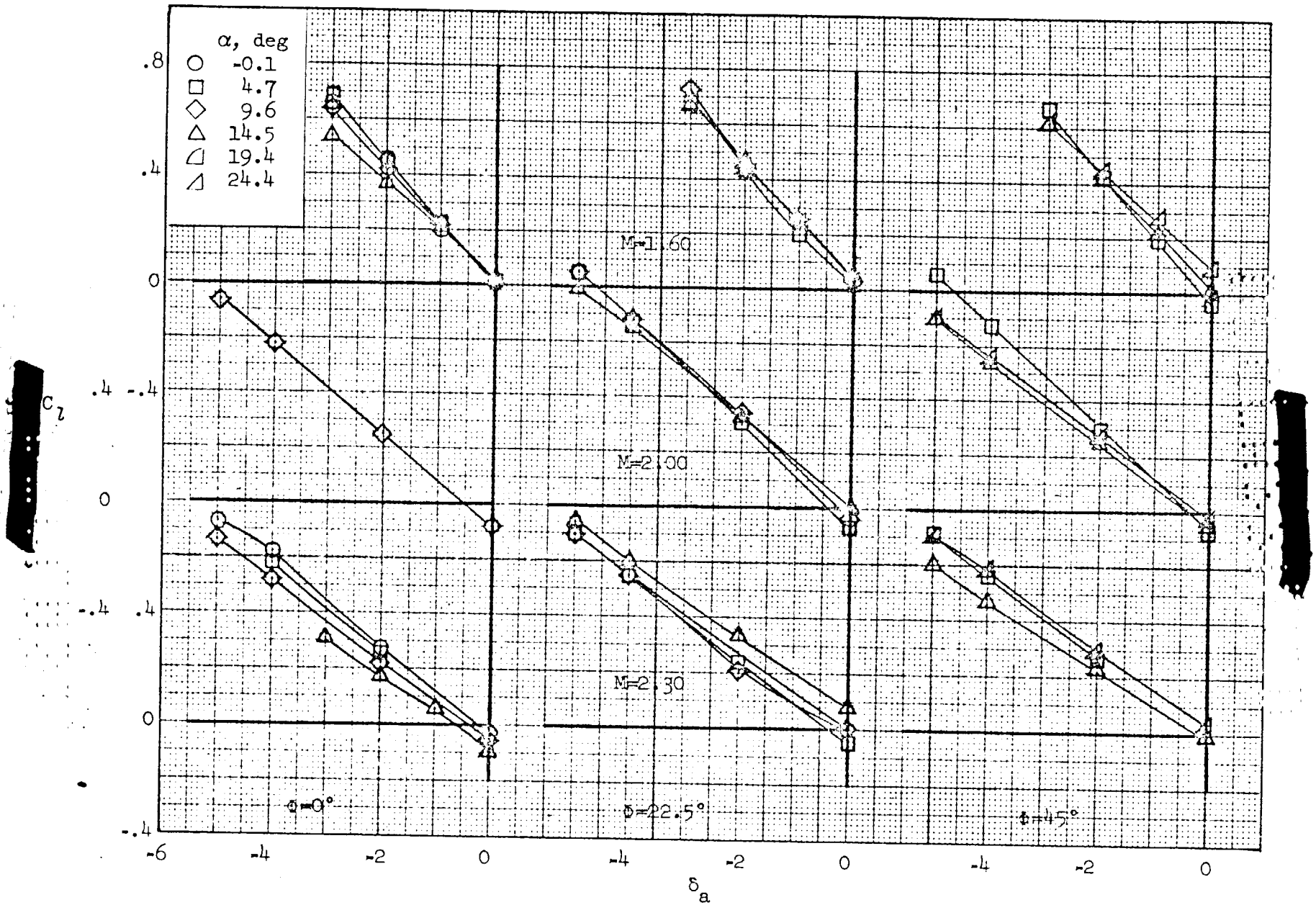

Figure 16.- The variation with control-surface-aileron deflection of rolling-moment coefficient. BWE configuration.

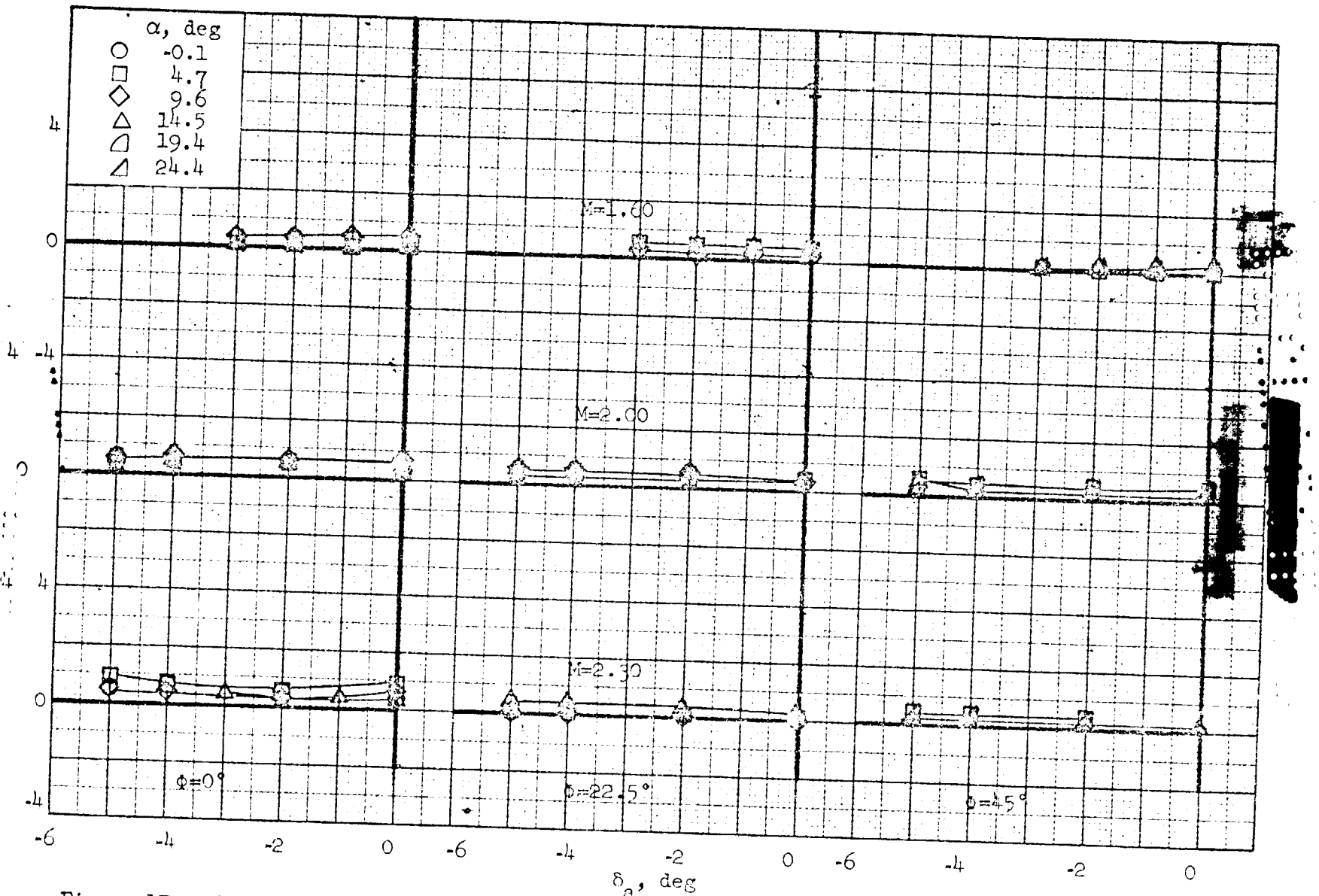

Figure 17.- The variation with control-surface-aileron deflection of pitching-moment coefficient. Total control-surface deflection δ_T set for trim. BWE configuration.